Cell Calcium 101 (2022) 102502

Contents lists available at ScienceDirect

Cell Calcium

journal homepage: www.elsevier.com/locate/ceca

Conjugated polymers mediate intracellular Ca^{2+} signals in circulating endothelial colony forming cells through the reactive oxygen species-dependent activation of Transient Receptor Potential Vanilloid 1 (TRPV1)

Sharon Negri [a], Pawan Faris [a,§], Gabriele Tullii [b,§], Mauro Vismara [a], Alessandro F. Pellegata [b,$], Francesco Lodola [b,#], Gianni Guidetti [a], Vittorio Rosti [c], Maria Rosa Antognazza [b,&,**], Francesco Moccia [a,&,*]

[a] Department of Biology and Biotechnology "Lazzaro Spallanzani", University of Pavia, 27100 Pavia, Italy
[b] Center for Nano Science and Technology@PoliMi, Istituto Italiano di Tecnologia, 20133 Milano, Italy
[c] Center for the Study of Myelofibrosis, Laboratory of Biochemistry, Biotechnology and Advanced Diagnosis, IRCCS Policlinico San Matteo Foundation, 27100 Pavia, Italy

ARTICLE INFO

Keywords:
Conjugated polymers
Optical stimulation
Endothelial colony forming cells
Transient receptor potential vanilloid 1
Reactive oxygen species

ABSTRACT

Endothelial colony forming cells (ECFCs) represent the most suitable cellular substrate to induce revascularization of ischemic tissues. Recently, optical excitation of the light-sensitive conjugated polymer, regioregular Poly (3-hexyl-thiophene), rr-P3HT, was found to stimulate ECFC proliferation and tube formation by activating the non-selective cation channel, Transient Receptor Potential Vanilloid 1 (TRPV1). Herein, we adopted a multidisciplinary approach, ranging from intracellular Ca^{2+} imaging to pharmacological manipulation and genetic suppression of TRPV1 expression, to investigate the effects of photoexcitation on intracellular Ca^{2+} concentration ($[Ca^{2+}]_i$) in circulating ECFCs plated on rr-P3HT thin films. Polymer-mediated optical excitation induced a long-lasting increase in $[Ca^{2+}]_i$ that could display an oscillatory pattern at shorter light stimuli. Pharmacological and genetic manipulation revealed that the Ca^{2+} response to light was triggered by extracellular Ca^{2+} entry through TRPV1, whose activation required the production of reactive oxygen species at the interface between rr-P3HT and the cell membrane. Light-induced TRPV1-mediated Ca^{2+} entry was able to evoke intracellular Ca^{2+} release from the endoplasmic reticulum through inositol-1,4,5-trisphosphate receptors, followed by store-operated Ca^{2+} entry on the plasma membrane. These data show that TRPV1 may serve as a decoder at the interface between rr-P3HT thin films and ECFCs to translate optical excitation in pro-angiogenic Ca^{2+} signals.

1. Introduction

Endothelial colony forming cells (ECFCs) represent the endothelial precursor subtype bearing the greatest potential to prompt vascular regeneration in ischemic disorders [1, 2]. Unlike myeloid angiogenic cells, such as colony forming unit endothelial cells and circulating angiogenic cells, ECFCs retain a truly endothelial phenotype, display high proliferative and clonogenic potential, may physically engraft within nascent vasculature as well as release pro-angiogenic mediators, and were shown to promote blood vessel regrowth and/or rescue local blood perfusion in multiple models of ischemic disorders [2–4]. The major hurdles that limit the application of autologous ECFCs in

* Corresponding author at: Department of Biology and Biotechnology "Lazzaro Spallanzani", Laboratory of General Physiology, University of Pavia, Via Forlanini 6, 27100, Pavia, Italy.
** Corresponding author at: Center for Nano Science and Technology@PoliMi, Istituto Italiano di Tecnologia, Via Giovanni Pascoli 70, 20133, Milano, Italy.
E-mail addresses: mariarosa.antognazza@iit.it (M.R. Antognazza), francesco.moccia@unipv.it (F. Moccia).
§ Equal contribution
$ Present address: Department of Chemistry, Materials and Chemical Engineering "Giulio Natta", Politecnico di Milano, 20133 Milano, Italy
# Present address: Department of Biotechnology and Biosciences, University of Milano Bicocca, 20126 Milano, Italy.
& These Authors share Senior Authorship and should be considered as co-last authors

https://doi.org/10.1016/j.ceca.2021.102502
Received 15 October 2021; Received in revised form 14 November 2021; Accepted 15 November 2021
Available online 19 November 2021

regenerative medicine are represented by their low frequency in peripheral circulation (~5–20 cells/100 mL blood) and the remarkable reduction in their vaso-reparative ability upon prolonged exposure to the most common risk factors, e.g., aging, hypertension, and obesity, which predispose to ischemic events [3, 4]. Multiple strategies were put forward to enhance the regenerative efficacy of circulating ECFCs, including ex vivo expansion to achieve therapeutically relevant cell numbers, and pharmacological or genetic manipulation of their pro-angiogenic signaling pathways [3–6]. Furthermore, circulating ECFCs can be recruited into sites of neovessel formation through the local injection of chemoattractants [7, 8]. All these approaches are certainly promising but cannot overcome some intrinsic limitations that may severely hamper their therapeutic application. For instance, transducing ECFCs with genes that stimulate angiogenesis, as well as the local delivery of bioactive cues to enhance their pro-angiogenic potential, display limited spatial resolution and do not permit temporally precise regulation of ECFCs' activity [3, 5, 9].

Geneless optical stimulation could provide an unprecedented spatio-temporal resolution, higher selectivity and lower invasiveness as compared to the existing genetic and pharmacological control strategies [9–12]. Among available photoactive materials, with proven photo-transduction efficiency within in vitro and/or in vivo environment, organic semiconductors represent a highly powerful strategy, which has been gaining increasing attention in the latest few years [10, 12, 13]. Conjugated polymers, in particular, constitute ideal artificial light transducers since they present an array of biophysical features that make them amenable for long-term biological applications [10, 12, 13]: (1) are mechanically flexible, ultrastretchable and solution processable; (2) exhibit low toxicity, are highly biocompatible and suitable to establish a seamless interface with biological tissues; (3) support both ionic and electronic conduction; and (4) are sensitive to visible light. Among others, regio-regular Poly (3-hexyl-thiophene), rr-P3HT, represents a workhorse nanomaterial for organic semiconductors that is widely employed to gain light-induced control of cellular activity [12–14]. For instance, the photostimulation of rr-P3HT thin films has been shown to induce changes in the membrane potential, i.e., depolarization followed by hyperpolarization, in non-excitable HEK-293 cells [15] and to modulate chloride channel conductance in primary rat neocortical astrocytes [16]. Furthermore, optical stimulation fired action potentials in primary rat hippocampal neurons cultured on rr-P3HT polymers [17] and induced contraction in human induced-pluripotent stem cells derived cardiomyocytes grown on the rr-P3HT interface [18]. Furthermore, optical excitation of rr-P3HT-based hybrid bioelectronic interfaces induced neuronal activity in both ex vivo brain slices [19] and retinal explants [20], and proved effective as a strategy to rescue light sensitivity and visual acuity in a rat model of degenerative blindness [21–23].

The non-selective cation channel Transient Receptor Potential Vanilloid 1 (TRPV1), which is mainly located on the plasma membrane, is nicely suited to integrate the chemical, e.g., nontoxic concentrations of reactive oxygen species (ROS) [24, 25], and physical, e.g. a local increase in temperature [15, 19], signals generated by rr-P3HT upon visible light excitation [9, 26, 27]. When TRPV1 opens at hyperpolarized membrane potentials, it carries an inward current that is a mixture of sodium and calcium ions [28, 29] and can deliver both electrical (i.e., membrane depolarization and activation of voltage-gated channels in excitable cells) and chemical (i.e., an increase in intracellular Ca^{2+} concentration or $[Ca^{2+}]_i$) signals to the hosting cell [9, 30]. While a number of reports clearly demonstrated that TRPV1 could provide the cellular switch that translates optical excitation of rr-P3HT into a bioelectrical signal [27, 31], the ensuing increase in $[Ca^{2+}]_i$ has never been evaluated. This issue is of compelling relevance as changes in $[Ca^{2+}]_i$ represent a widespread mechanism that regulates a plethora of cellular functions [32, 33] and the finely tuned control of cellular activity through spatio-temporally regulated Ca^{2+} signals stands among the most promising alternative strategies to precisely control cell fate [6, 34-43]. Intriguingly, a recent investigation revealed that optical excitation of circulating ECFCs cultured on rr-P3HT thin films stimulates proliferation and tube formation, which are the two main mechanisms underlying tissue revascularization [3], upon TRPV1 activation [31]. Herein, we adopted a multidisciplinary approach, ranging from imaging of intracellular Ca^{2+} dynamics to pharmacological manipulation and genetic suppression of TRPV1 expression, to investigate the effects of visible light on $[Ca^{2+}]_i$ in ECFCs plated on rr-P3HT. We provided the first evidence that optical stimulation of rr-P3HT results in TRPV1-mediated intracellular Ca^{2+} signals, which may adopt either an oscillatory or non-oscillatory pattern and are directly triggered by ROS. These data clearly show that TRPV1 may serve as a decoder at the interface between rr-P3HT thin films and ECFCs to translate the illumination with visible light in pro-angiogenic Ca^{2+} signals that can be effectively used to regenerate the vascular network of ischemic tissues.

2. Materials and methods

2.1. Polymer thin films preparation

Poly-3-Hexyl-Thiophene (P3HT) polymer (15,000–45,000 MW, purchased from Sigma Aldrich (Merk Millipore, Darmstadt, Germany) and used without further purification) was dissolved in Chlorobenzene up to a final concentration of 20 mg/mL. The solution was stirred at 65 °C for 6 h . Glass substrates were carefully cleaned before use, by subsequent rinses in ultrasonic bath with deionized water, acetone, isopropanol (10 min each). P3HT solution was spin coated (1500 rpm for 1 min) on the glass substrates, obtaining a final thickness of 130 nm and an optical density of 0.6 (at the main absorption peak). Glass/P3HT samples used as cell culturing substrates were thermally sterilized (2 h, 120 °C).

2.2. Isolation and cultivation of ECFCs

Blood samples (40 ml) collected in EDTA (ethylenediaminetetraacetic acid)-containing tubes were obtained from healthy human volunteers aged from 22 to 28 years old. The Institutional Review Board at "Istituto di Ricovero e Cura a Carattere Scientifico Policlinico San Matteo Foundation" in Pavia approved all protocols and specifically approved this study. Informed written consent was obtained according to the Declaration of Helsinki of 1975 as revised in 2008. To isolate ECFCs, mononuclear cells (MNCs) were separated from peripheral blood by density gradient centrifugation on lymphocyte separation medium for 30 min at 400 g and washed twice in endothelial basal medium-2 (EBM-2) with 2% foetal bovine serum (FBS). A median of 36×10^6 MNCs (range 18–66) were plated on collagen-coated culture dishes (BD Biosciences) in the presence of the endothelial cell growth medium EGM-2 MV Bullet Kit (Lonza) containing EBM-2, 5% FBS, recombinant human (rh) EGF, rh-VEGF, rh-FGF-B, rh-IGF-1, ascorbic acid, and heparin, and maintained at 37 °C in 5% CO_2 and humidified atmosphere. Discard of non-adherent cells was performed after 2 days; thereafter medium was changed three times a week. The outgrowth of endothelial colonies from adherent MNCs was characterized by the formation of a cluster of cobblestone-appearing cells, resembling endothelial cells. That ECFCs-derived colonies belonged to endothelial lineage was confirmed as described in [44, 45].

2.3. Solutions

Physiological salt solution (PSS) had the following composition (in mM): 150 NaCl, 6 KCl, 1.5 $CaCl_2$, 1 $MgCl_2$, 10 Glucose, 10 Hepes. In Ca^{2+}-free solution ($0Ca^{2+}$), Ca^{2+} was substituted with 2 mM NaCl, and 0.5 mM EGTA was added. Solutions were titrated to pH 7.4 with NaOH. The osmolality of PSS as measured with an osmometer (Wescor 5500, Logan, UT) was 338 mmol/kg.

2.4. $[Ca^{2+}]_i$ measurements

ECFCs, plated either on glass/P3HT or bare glass substrates, were loaded with 4 μM fura-2 acetoxymethyl ester (fura-2/AM; 1 mM stock in dimethyl sulfoxide) in PSS for 1 h at room temperature. After washing in PSS, the sample was fixed to the bottom of a Petri dish and the cells observed by an upright epifluorescence Axiolab microscope (Carl Zeiss, Oberkochen, Germany), usually equipped with a Zeiss × 40 Achroplan objective (water-immersion, 2.0 mm working distance, 0.9 numerical aperture). ECFCs were excited alternately at 340 and 380 nm, and the emitted light was detected at 510 nm. A first neutral density filter (1 or 0.3 optical density) reduced the overall intensity of the excitation light, and a second neutral density filter (optical density = 0.3) was coupled to the 380 nm filter to approach the intensity of the 340 nm light. A round diaphragm was used to increase the contrast. The excitation filters were mounted on a filter wheel (Lambda 10, Sutter Instrument, Novato, CA, USA). Custom software, working in the LINUX environment, was used to drive the camera (Extended-ISIS Camera, Photonic Science, Millham, UK) and the filter wheel, and to measure and plot on-line the fluorescence from 10 up to 30 rectangular "regions of interest" (ROI). Each ROI was identified by a number. Since cell borders were not clearly identifiable, a ROI may not include the whole cell or may include part of an adjacent cell. Adjacent ROIs never superimposed. To provide polymer photoexcitation, an external light emitting diode was employed (THORLABS M470L4-C5, Newton, New Jersey, USA), with spectral emission centered around 470 nm, which is far away from Fura-2 light absorption spectra, and photoexcitation impinging on the sample from the glass substrate side with a power density 0.6 mW/mm^2. Light pulses of different duration, in the range 2.5–20 sec, were used to optically stimulate the P3HT polymer films as well as the uncovered, control glass substrates. During photoexcitation protocol, the acquisition system was off, and this is indicated by the corresponding upward/downward deflection of the Ca^{2+} tracings at the time of illumination. On/off switching time are in the order of ms, thus not interfering with the monitoring of $[Ca^{2+}]_i$ dynamics. $[Ca^{2+}]_i$ was monitored by measuring, for each ROI, the ratio of the mean fluorescence emitted at 510 nm when exciting alternatively at 340 and 380 nm (F_{340}/F_{380}). An increase in $[Ca^{2+}]_i$ causes an increase in the ratio [44]. Ratio measurements were performed and plotted on-line every 3 s and were never longer than 3600 sec. In the figures, each Ca^{2+} tracing refers to an individual cell and is representative of at least three independent experiments. The experiments were performed at room temperature (22 °C).

2.5. rr-P3HT fluorescence emission measurements

GLASS/ P3HT samples were immersed in PSS extracellular medium and the fluorescence at the polymer surface was acquired in different field of views (excitation/emission wavelengths, 520/660 nm; integration time, 100 ms; binning:2 × 2) using an upright microscope (Olympus BW63), equipped with a 20X water immersion objective and a sCMOS Camera (Prime BSI, Teledyne Photometrics; Tucson, Arizona, USA). Then, the Fura-2/AM optical excitation protocol, described in Section 2.4, was applied to the same field of views. Some fields were not treated as control. The P3HT fluorescence emission was measured again in the same areas. The fluorescence intensity was evaluated over Regions of Interest placed inside the treated/untreated regions, using ImageJ software. Mean values were averaged over 4 fields of view, over 3 statistically independent samples.

2.6. SDS-PAGE and immunoblotting

Cells were lysed in ice-cold RIPA buffer (50 mM TRIS/HCl, pH 7.4, 150 mM NaCl, 1% Nonidet P40, 1 mM EDTA, 0.25% sodium deoxycholate, 0.1% SDS) added of protease and phosphatase inhibitors. Upon protein quantification, the samples were dissociated by addition of half volume of SDS-sample buffer 3X (37.5 mM TRIS, pH 8.3, 288 mM glycine, 6% SDS, 30% glycerol, and 0.03% bromophenol blue), separated by SDS-PAGE on a 7.5% polyacrylamide gel, and blotted on a PVDF membrane. Membrane probing was performed using the different antibodies diluted 1:1000 in TBS (20 mM Tris, 500 mM NaCl, pH 7.5) containing 5% BSA and 0.1% Tween-20 in combination with the appropriate HRP-conjugated secondary antibodies (1:2000 in PBS plus 0.1% Tween-20). The following antibodies were used: anti-TRPV1 (ab3487) from ABCAM (Cambridge,UK) and anti-Tubulin (sc-32,293) from Santa Cruz Biotechnology (Dallas, Texas, USA) as equal loading control. The chemiluminescence reaction was performed using Immobilon Western (Millipore) and images were acquired by Chemidoc XRS (Bio-Rad, Segrate, Mi, Italy).

2.7. Gene silencing

A selective siRNA, targeting human TRPV1, was purchased by Sigma-Aldrich Inc. MISSION esiRNA (hTRPV1, EHU073721). Scrambled siRNA was used as negative control (defined as Ctrl in the Figures). Briefly, once the monolayer cells had reached 50% confluency, the medium was removed, and the cells were added with Opti-MEM I reduced serum medium without antibiotics (Life Technologies). siRNAs (100 nM final concentration) were diluted in Opti-MEM I reduced serum medium and mixed with Lipofectamine™ RNAiMAX transfection reagent (Invitrogen) prediluted in Opti-MEM), according to the manufacturer's instructions. After 20 min incubation at room temperature, the mixes were added to the cells and incubated at 37 °C for 5 h. Transfection mixes were then completely removed, and fresh culture media was added. The effectiveness of silencing was determined by immunoblotting (see Figure S2), and the silenced cells were used 48 h after transfection.

2.8. Intracellular reactive oxygen species detection

2′,7′-dichlorodihydrofluorescein diacetate (H_2DCF–DA, purchased from Sigma Aldrich) was employed for intracellular detection of Reactive Oxygen Species (ROS). ECFCs cultured on Glass/P3HT and glass control samples were photo-excited for 2.5 or 20 s from glass side with a LED system (Thorlabs M470L3-C5, λ = 470 nm, P = 0.6 mW/mm^2), thus employing the same parameters used for photoexcitation in $[Ca^{2+}]_i$ dynamics measurements. Subsequently, cells were incubated with the ROS probe for 30 min in PSS (10 μM). After careful wash-out of the excess probe from the extracellular medium, the fluorescence of the probes was recorded (excitation/emission wavelengths, 490/520 nm; integration time, 350 ms) with an upright microscope [Olympus BW63; Olympus Italia, Segrate (Mi), Italy], equipped with a 20X water immersion objective and a sCMOS Camera (Prime BSI, Teledyne Photometrics; Tucson, Arizona, USA). Variation of fluorescence intensity was evaluated over Regions of Interest covering single cells areas, and reported values represent the average over multiple cells (n > 400) belonging to 3 statistically independent samples. Image processing was carried out with ImageJ and subsequently analysed with Origin Pro 2018.

2.9. Statistics

All the data have been collected from ECFCs deriving from at least three coverslips from three independent experiments. The amplitude of the maximum variation in $[Ca^{2+}]_i$ induced by optical stimulation was measured as the difference between the maximum increase in F_{340}/F_{380} ratio and the mean ratio of 1 min baseline before the onset of the Ca^{2+} response. The amplitude of the 1st Ca^{2+} transient of the intracellular Ca^{2+} oscillations was measured as the difference between the Ca^{2+} peak and mean ratio of 1 min baseline before the Ca^{2+} peak. Oscillation frequency was calculated by dividing the number of Ca^{2+} transients by the duration of the recording after the light stimulus (40–45 min). The amplitude of Ca^{2+} signals induced by chemical stimulation (i.e.,

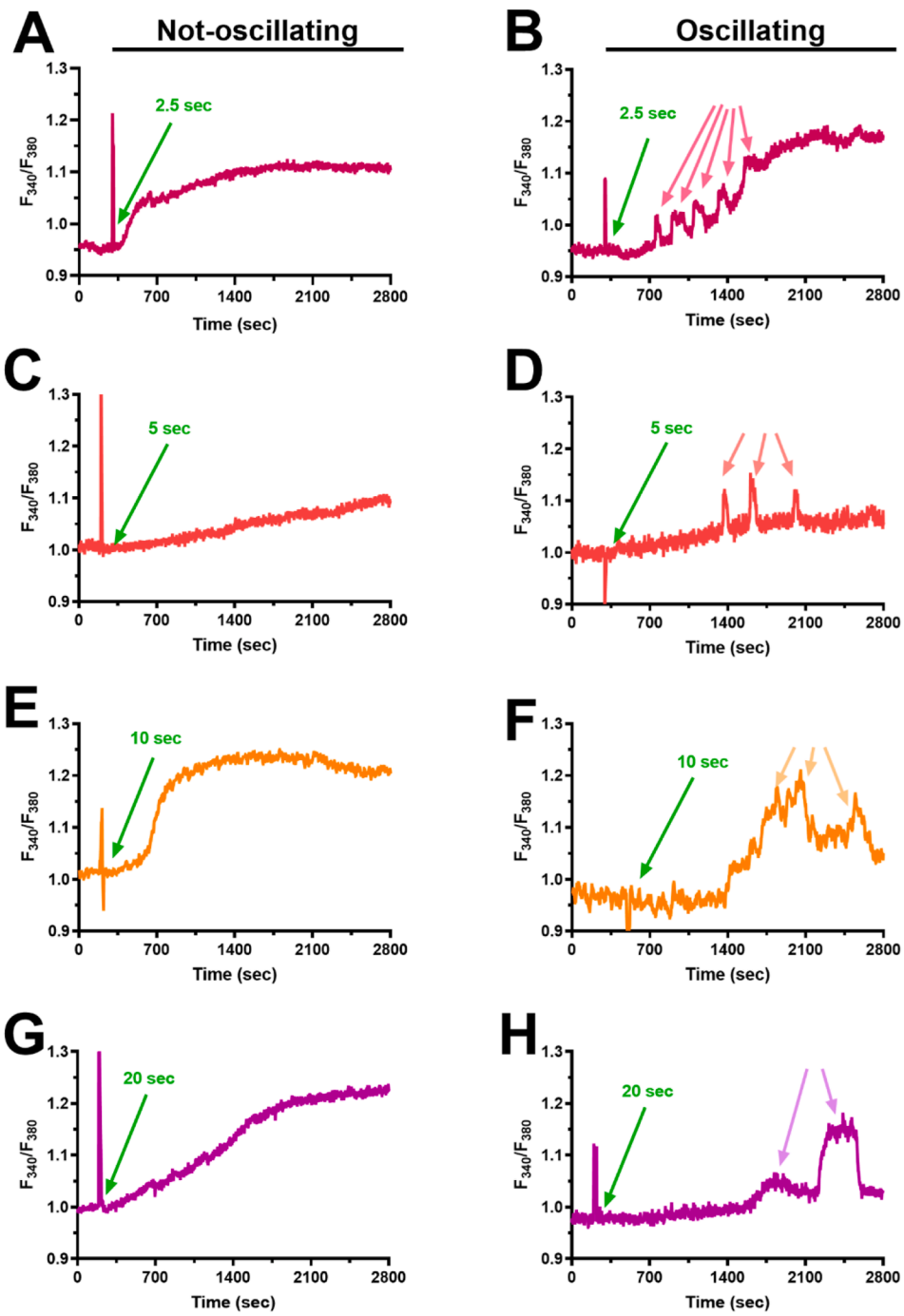

Fig. 1. Optical stimulation of rr-P3HT thin films induces an increase in $[Ca^{2+}]_I$ in circulating ECFCs. A. 2.5 sec of light stimulation elicited an increase in $[Ca^{2+}]_i$ characterized by a slowly rising signal in ≈60% ECFCs. B. Ca^{2+} oscillations evoked by 2.5 sec of optical stimulation in ≈40% ECFCs. C. Slowly rising Ca^{2+} signal induced by 5 sec long light pulse in ≈77% ECFCs. D. ≈23% displayed oscillations evoked by 5 sec of light stimulation. E. 10 sec of optical stimulation evoked a plateauing increase in $[Ca^{2+}]_i$ in ≈86%. F. Ca^{2+} oscillations stimulated by 10 sec long light pulses in ≈14%. G. 20 sec of light stimulation elicited a plateauing increase in $[Ca^{2+}]_i$ in ≈94%. H. ≈6% ECFCs displayed Ca^{2+} oscillations in response to 20 sec light pulse long stimulation.

capsaicin, hydrogen peroxide, and NADH) was measured as the difference between the difference between the maximum variation in $[Ca^{2+}]_i$ and the mean ratio of 1 min baseline before the Ca^{2+} peak. Pooled data are given as mean±SEM and statistical significance (P value) was evaluated by the Student's *t*-test for unpaired observations and by the one-way ANOVA test followed by the post-hoc Dunnett's or Bonferroni test, as appropriate. Data are presented as mean ± SEM, while the number of cells analysed is indicated in histogram bars or in the text.

2.10. Chemicals

Fura-2/AM was obtained from Invitrogen (Life Technologies Europe BV, Bleiswijk, ZUID-HOLLAND, Netherlands). All the chemicals were of analytical grade were obtained from Sigma Aldrich (Merk Millipore, Darmstadt, Germany), except BTP-2, obtained from Calbiochem (Merk Millipore, Darmstadt, Germany) and Xestospongin C (XeC) obtained from ABCAM (Cambridge, UK).

3. Results

3.1. Optical excitation of rr-P3HT thin films induces a complex increase in $[Ca^{2+}]_i$ in circulating ECFCs

In the absence of photostimulation, circulating ECFCs loaded with the Ca^{2+}-sensitive fluorophore, fura-2/AM (4 μM), did not display spontaneous Ca^{2+} oscillations, either when they were plated on uncoated glass coverslips or glass/P3HT samples (data not shown). Visible light pulses (wavelength excitation peak, 470 nm; photoexcitation

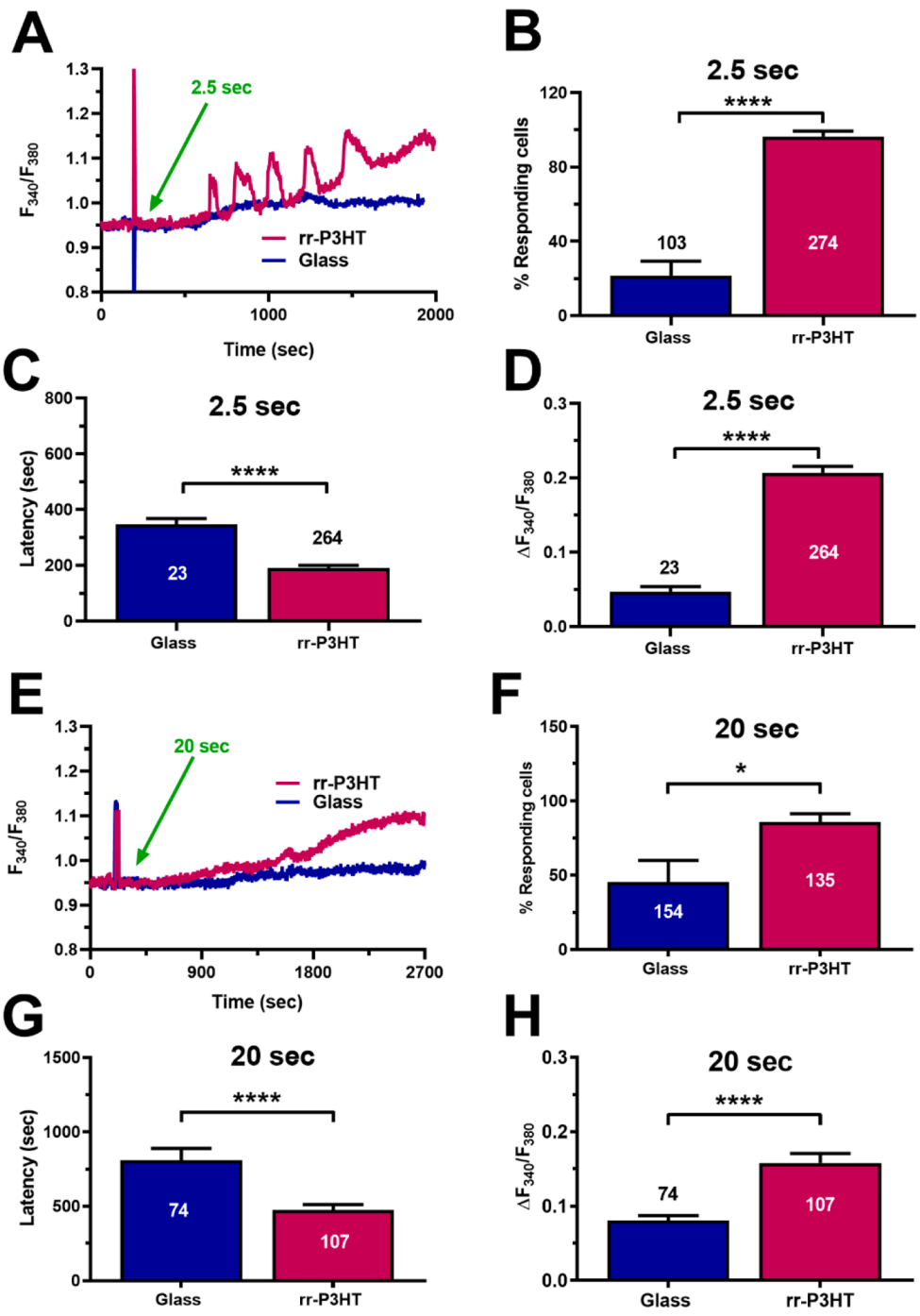

Fig. 2. Optical stimulation of glass coverslips does not reliably induce long-lasting elevations in $[Ca^{2+}]_i$ in ECFCs. A. 2.5 sec light pulse photoexcitation induced a faster and higher Ca^{2+} response in ECFCs plated on rr-P3HT as compared to ECFCs plated on glass coverslips. B. Mean ± SEM of the percentage of ECFCs displaying a Ca^{2+} response to 2.5 sec long light pulses in cells plated on glass coverslips and on rr-P3HT. C. Mean ± SEM of the latency of the response evoked by 2.5 sec long light pulses in ECFCs, respectively, cultured on glass coverslips and rr-P3HT thin films. D. Mean ± SEM of the amplitude of the Ca^{2+} responses to 2.5 sec long light pulses measured in ECFCs, respectively, cultured on glass coverslips and rr-P3HT thin films. E. 20 sec long light pulse evoked faster and higher intracellular Ca^{2+} signals in ECFCs plated on rr-P3HT compared to cells plated on glass coverslips. F. Mean ± SEM of the percentage of ECFCs displaying a Ca^{2+} responses to 20 sec long light pulses in the presence of glass coverslips and rr-P3HT thin films. G. Mean ± SEM of the latency of the response evoked by 10 sec long light pulses in ECFCs, respectively, cultured on glass coverslips and rr-P3HT thin films. H. Mean±SEM of the amplitude of the Ca^{2+} responses to 20 sec long light pulses measured in ECFCs, respectively, cultured on glass coverslips and rr-P3HT thin films. **** indicate $p < 0.0001$, while * indicates $p < 0.05$.

density, 0.6 mW/mm^2) were provided by a LED source incident from the glass side [27, 31]. Light pulses of different durations (2.5–20 sec) at the same photoexcitation density were delivered to ECFCs plated on rr-P3HT and loaded with fura-2A/AM and the changes in $[Ca^{2+}]_i$ were measured after termination of the illumination protocol. The Fura-2/AM optical stimulation protocol, with excitation wavelength at 340/380 nm, presents a negligible overlap with the rr-P3HT optical absorption (Figure S1A) and does not lead to degradation of the rr-P3HT thin film optical properties, as carefully verified by measuring its intrinsic fluorescence emission. No sizable differences were observed in the same region before and after exposure to the Fura-2/AM excitation (Figure S1B). A long-lasting increase in $[Ca^{2+}]_i$ was evoked in the majority of ECFCs subjected to photoexcitation for ≥ 2.5 sec (Fig. 1). Upon 2.5 sec illumination (Fig. 1A), almost half of ECFCs (60.95%, $n = 167$) displayed a slowly progressing increase in $[Ca^{2+}]_i$ to a plateau level, which remained stable above the baseline until the end of the recording (Fig. 1A). We term this mode of Ca^{2+} signaling induced by photoexcitation as "not-oscillating" signal. In the remaining fraction of ECFCs (39.05%, $n = 107$), a 2.5 sec light pulse evoked complex Ca^{2+} waveforms (Fig. 1B). The gradual rise in $[Ca^{2+}]_i$ was indeed overlapped by rapid Ca^{2+} spikes that terminated before the plateau level was achieved (Fig. 1B). These fluctuations in $[Ca^{2+}]_i$ present the fast kinetics of baseline Ca^{2+} spikes, but each of them falls to a $[Ca^{2+}]_i$ level that is increasingly above the resting baseline. Therefore, we term this mode of Ca^{2+} signaling induced by photoexcitation as "oscillating" [46–48]. Notably, there was no significant difference in the amplitude of the plateau level above the resting baseline that was achieved by the $[Ca^{2+}]_i$ in "not-oscillating" vs. "oscillating" cells (0.199±0.011, $n = 157$, and

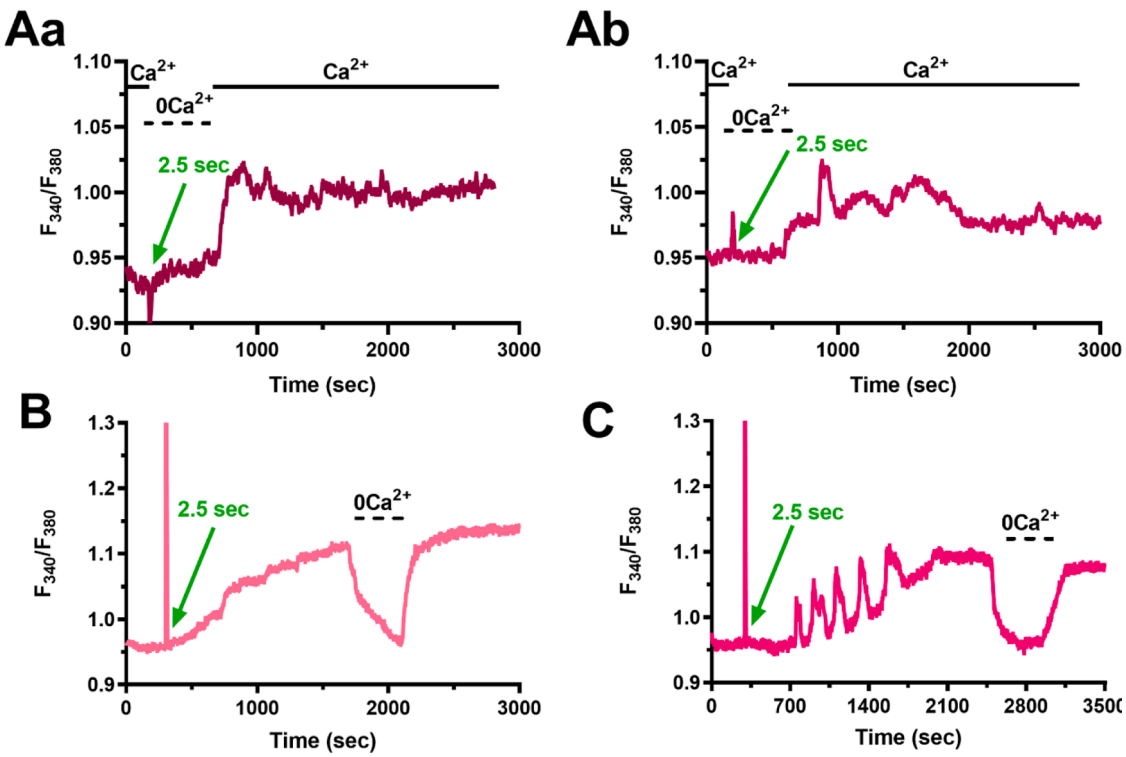

Fig. 3. Extracellular Ca^{2+} entry triggers and maintains the Ca^{2+} response induced in ECFCs by photoexcitation of rr-P3HT thin films. A. ECFCs subjected to 2.5 sec long light pulses in the absence of extracellular Ca^{2+} did not show any increase in $[Ca^{2+}]_i$ over 300 sec. Restoration of extracellular Ca^{2+} in the bath resulted in a rapid increase in $[Ca^{2+}]_i$ that could display a plateauing (Aa) or an oscillatory pattern (Ab). B. Removal of extracellular Ca^{2+} during the plateau phase caused a prompted and reversible reduction of $[Ca^{2+}]_i$ to the baseline in plateauing cells. C. Removal of extracellular Ca^{2+} caused a prompted and reversible reduction of $[Ca^{2+}]_i$ to the baseline also in oscillating cells.

0.219±0.012, $n = 107$).

The percentage of ECFCs displaying an oscillatory Ca^{2+} signal progressively decreased upon illumination with longer light pulses (5–20 sec). Intracellular Ca^{2+} oscillations appeared in 22.55% ($n = 102$), 14.45% ($n = 152$), and 5.63% ($n = 142$) ECFCs subjected to photoexcitation for, respectively, 5 sec, 10 sec, and 20 sec, with the remaining cells displaying a non-oscillating Ca^{2+} signal (Fig. 1). Although the latency of the Ca^{2+} response was significantly ($p < 0.05$) shorter in response to 2.5 sec light pulses (Figure S2A), the amplitude of the maximum variation that $[Ca^{2+}]_i$ achieved, either directly or after the oscillations, remained constant for each stimulus duration (Figure S2B). In oscillating ECFCs, the average amplitude of the first Ca^{2+} transient did not significantly change by varying the duration of photoexcitation (Figure S2C), while the oscillation frequency was significantly higher upon 2.5 sec long light pulses (Figure S2D).

The onset of multiple patterns of intracellular Ca^{2+} signals upon polymer-mediated photoexcitation is therapeutically relevant as heterogeneous increases in $[Ca^{2+}]_i$ can stimulate pro-angiogenic activity in both vascular endothelial cells [49–51] and circulating ECFCs [45, 52, 53]. Therefore, the bare impact of photoexcitation on intracellular Ca^{2+} dynamics was assessed by using control, glass substrates. Under these conditions, only a minority of ECFCs subjected to a 2.5 sec long light pulse displayed a slowly activating, non-oscillating Ca^{2+} signal (Fig. 2A and Fig. 2B, 20% vs. 95%), which displayed a significantly ($p < 0.05$) longer latency (Fig. 2C) and a significantly lower peak amplitude (Fig. 2D) as compared to the cells cultured on rr-P3HT. Intracellular Ca^{2+} oscillations were never induced by optical stimulation in ECFCs cultured on light-transparent substrates. Similar findings were obtained by increasing stimulus duration to 20 sec (Fig. 2E–Fig. 2H). Taken together, these data indicate that polymer-mediated optical stimulation selectively results in an increase in $[Ca^{2+}]_i$, which can adopt multiple pro-angiogenic waveforms.

3.2. The role of extracellular Ca^{2+} entry in the Ca^{2+} response evoked by polymer-mediated optical excitation

Intracellular Ca^{2+} signaling in circulating ECFCs may be triggered by the opening of Ca^{2+}-permeable channels that are located either in the plasma membrane or in intracellular organelles [54, 55]. In order to assess the Ca^{2+} source that triggers the Ca^{2+} response to optical stimulation, ECFCs were loaded with Fura-2/AM and then subjected to 2.5 sec long light pulses upon removal of extracellular Ca^{2+} ($0Ca^{2+}$). Fig. 3A shows that, under such conditions, photoexcitation did not elicit any robust increase in $[Ca^{2+}]_i$ over 300 sec, a time interval that is remarkably longer of the average latency of the Ca^{2+} response elicited by this protocol (i.e., 220.0 ± 11 sec, see Fig. 2A). Restitution of extracellular Ca^{2+} to the perfusate resulted in a prompt increase in $[Ca^{2+}]_i$, which could display either a non-oscillatory (Fig. 3Aa) or an oscillatory pattern (Fig. 3Ab). The role of extracellular Ca^{2+} in maintaining the Ca^{2+} signal initiated by photoexcitation was then assessed by removing extracellular Ca^{2+} during the plateau phase. This maneuver caused a prompted and reversible reduction of $[Ca^{2+}]_i$ to the baseline (Fig. 3B, non-oscillating response, and Fig. 3C, oscillatory response). These data, therefore, demonstrate that extracellular Ca^{2+} entry triggers and maintains the Ca^{2+} response to polymer-mediated photoexcitation in circulating ECFCs.

3.3. TRPV1 is expressed and mediates extracellular Ca^{2+} entry in ECFCs

A recent investigation by our group provided the strong evidence that photoexcitation induced TRPV1-mediated depolarization in circulating ECFCs growing on rr-P3HT thin films [31]. This study, however, did not assess whether TRPV1 protein is expressed and mediates an increase in $[Ca^{2+}]_i$ in ECFCs. Immunoblotting revealed a major band of ≈100 kDa, which is the predicted molecular weight of TRPV1 [28]

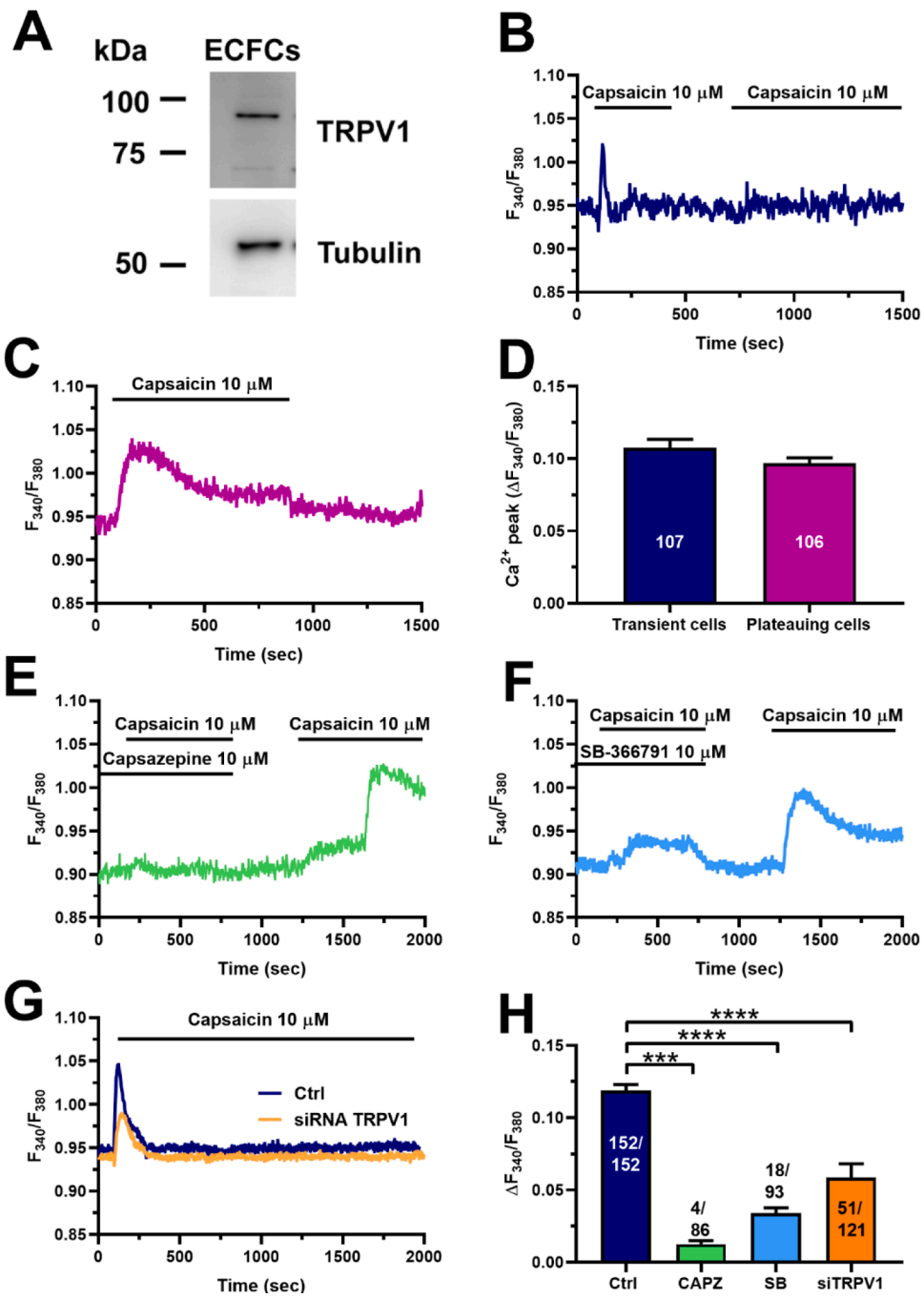

Fig. 4. TRPV1 is expressed and mediated extracellular Ca^{2+} entry in ECFCs. A. TRPV1 protein expression was detected by immunoblotting analysis in ECFCs. B. Capsaicin (10 μM), a selective TRPV1-agonist, induced a fast and transient increase in $[Ca^{2+}]_i$ in 107 of 213 cells. C. Capsaicin (10 μM) induced a biphasic Ca^{2+} signal, which decayed to the baseline upon the washout of the agonist from the perfusate, in 106 of 213 cells. D. Mean±SEM of the amplitude of the two different types of the Ca^{2+} response. E. The competitive TRPV1 antagonist, capsazepine (10 μM, 30 min), dramatically affected the amplitude of capsaicin-induced Ca^{2+} signals. Subsequent administration of capsaicin (10 μM), after washout of the antagonist, induced a prompted increase in $[Ca^{2+}]_i$. F. SB-366,791 (10 μM, 30 min), a structurally different TRPV1 antagonist, strongly reduced the Ca^{2+} response induced by capsaicin (10 μM). G. Genetic silencing of TRPV1 through the specific siTRPV1 significantly reduced the Ca^{2+} response to capsaicin (10 μM). H. Mean±SEM of the amplitude of the capsaicin-induced Ca^{2+} response under the designated treatments, i.e., in the presence of capsazepine (CAPZ) or SB-366,791 (SB) or upon gene silencing of TRPV1 (siTRPV1). **** indicate $p < 0.0001$, while *** indicate $p < 0.001$.

(Fig. 4A). We then assessed the effect of capsaicin, a selective TRPV1 agonist [28, 56, 57], on $[Ca^{2+}]_i$. Capsaicin (10 μM) evoked a fast Ca^{2+} transient in 107 out of 213 cells (50.2%) (Fig. 4B). Subsequent delivery of this dietary agonist failed to evoke a detectable increase in $[Ca^{2+}]_i$ (Fig. 4B), which suggests that the Ca^{2+} response to capsaicin rapidly desensitized in these cells [9, 57]. In the remaining 106 cells (49.8%), capsaicin (10 μM) induced a biphasic Ca^{2+} signal, which decayed to the baseline upon washout of the agonist from the bath, (Fig. 4C). The biphasic Ca^{2+} response to capsaicin consisted in an initial Ca^{2+} peak which then declined to a steady-state plateau level that persisted as long as the agonist was presented to the cells. This heterogeneous pattern of Ca^{2+} response to capsaicin has been reported in other cell types [57–59]. However, there was no significant difference in the Ca^{2+} peak amplitude of the two distinct Ca^{2+} signals evoked by capsaicin (Fig. 4D).

In order to confirm that TRPV1 mediates an increase in $[Ca^{2+}]_i$, we probed the effects of two structurally unrelated compounds, such as capsazepine and SB-366,791, which are recognized as selective blockers of TRPV1 [9, 27, 56, 57, 60, 61]. The Ca^{2+} response to capsaicin (10 μM) was reversibly blocked either by capsazepine (10 μM, 30 min) (Fig. 4E) or by SB-366,791 (10 μM, 30 min) (Fig. 4F). Furthermore, genetic silencing of TRPV1 protein through a specific small interfering RNA (siTRPV1) also impaired capsaicin-induced intracellular Ca^{2+} signals in ECFCs (Fig. 4G). The efficacy of this treatment to down-regulate TRPV1 expression has been confirmed by immunoblotting (Figure S3), whereas the impact of the pharmacological and genetic manipulation of TRPV1 has been summarized in Fig. 4H). In aggregate, these findings demonstrate that TRPV1 is able to trigger an increase in $[Ca^{2+}]_i$ in circulating ECFCs.

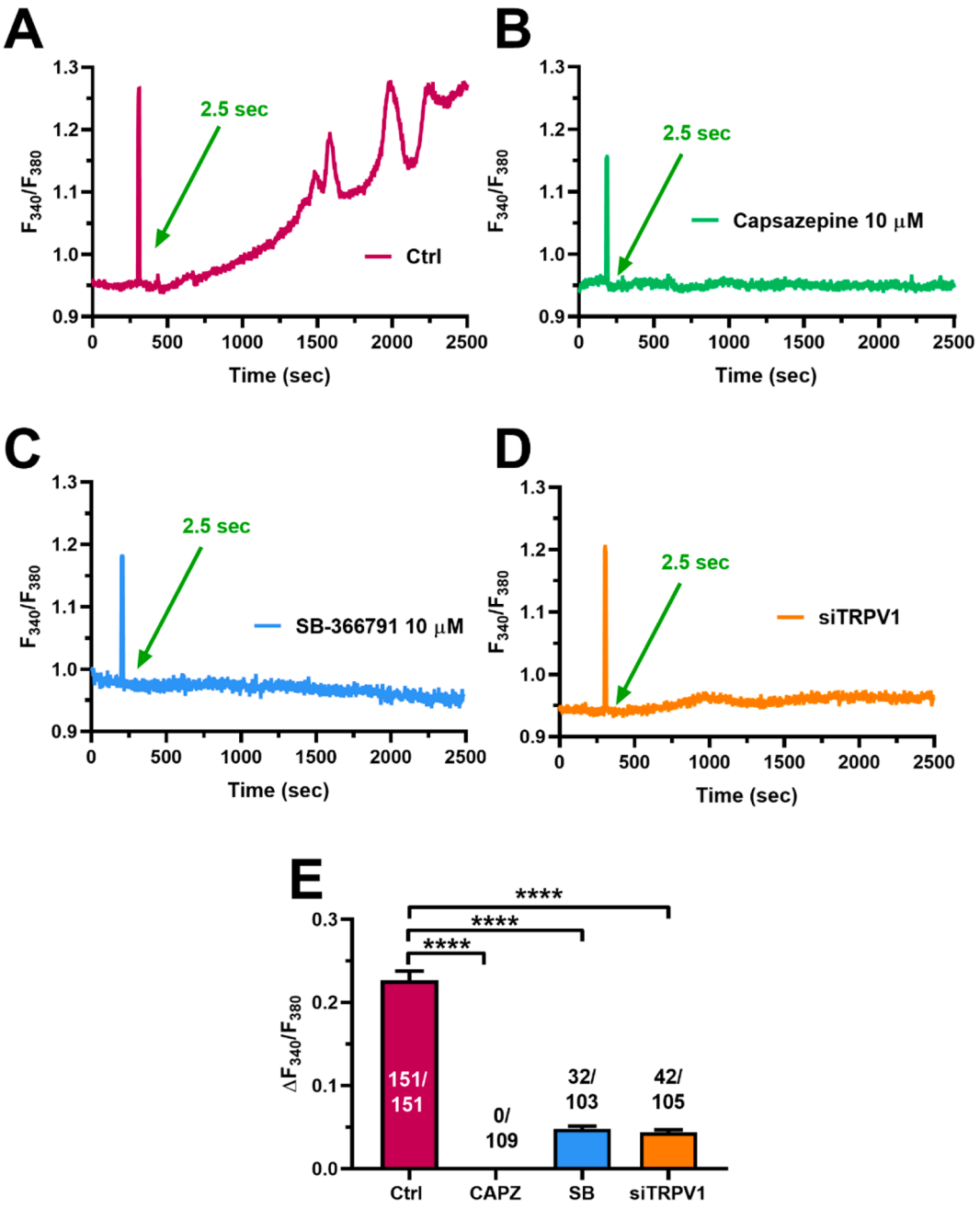

Fig. 5. TRPV1 mediates light-induced Ca^{2+} signals in ECFCs plated on rr-P3HT thin films. A. 2.5 sec light pulse induced an oscillatory Ca^{2+} response in ECFCs plated on rr-P3HT and not pretreated with TRPV1 inhibitors. B. Pharmacological inhibition of TRPV1 with capsazepine (10 μM, 30 min) completely abrogated the Ca^{2+} response to optical stimulation. C. SB-366,791 (10 μM, 30 min) strongly inhibited the Ca^{2+} signal induced by photoexcitation. D. Light-induced increase in $[Ca^{2+}]_i$ was dramatically reduced by genetic silencing of TRPV1 through the specific siTRPV1. E. Mean ± SEM of the amplitude of the Ca^{2+} response in cells under the designated treatments, i.e., in the presence of capsazepine (CAPZ) or SB-366,791 (SB) or upon gene silencing of TRPV1 (siTRPV1). **** indicate $p < 0.0001$.

3.4. TRPV1 triggers the complex increase in $[Ca^{2+}]_i$ induced by polymer-mediated optical excitation in ECFCs

We exploited the pharmacological and genetic approach described above to assess whether TRPV1 initiates the Ca^{2+} response induced in ECFCs by the optical excitation of rr-P3HT thin films. Fig. 5A shows the complex increases in $[Ca^{2+}]$ evoked by a 2.5 sec excitation pulse in ECFCs maintained under control conditions. The Ca^{2+} response to photoexcitation was suppressed by pharmacological blockade of TRPV1 with either capsazepine (10 μM, 30 min) (Fig. 5B) or SB-366,791 (10 μM, 30 min) (Fig. 5C). Likewise, genetic deletion of TRPV1 impaired light-induced intracellular Ca^{2+} signals in circulating ECFCs (Fig. 5D). The statistical analysis of these data has been reported in Fig. 5E. Parallel recordings confirmed that the Ca^{2+} response to capsaicin (10 μM) was not dampened by culturing ECFCs on rr-P3HT thin films (Figure S4). Taken together, these findings demonstrate for the first time that TRPV1 activation triggers the complex increase in $[Ca^{2+}]_i$ induced by polymer-mediated optical excitation in circulating ECFCs.

3.5. The phototransduction mechanism: the role of ROS in the Ca^{2+} response to polymer-mediated optical excitation of rr-P3HT

A recent report by our groups suggested that the pro-angiogenic effect of rr-P3HT thin films is mainly mediated by ROS rather than heat

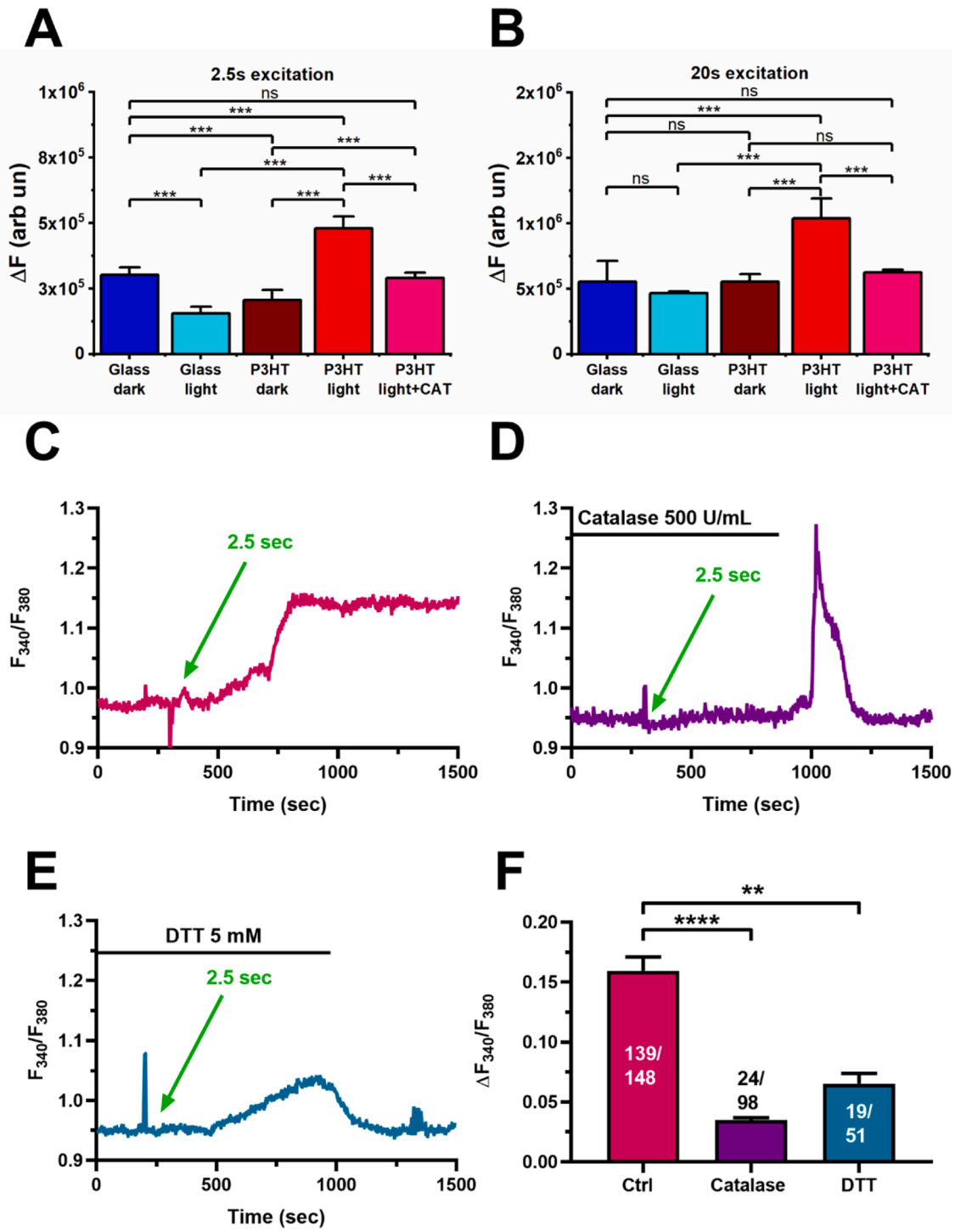

Fig. 6. The crucial role of ROS in the light-induced Ca^{2+} response in ECFCs plated on rr-P3HT. A. ECFCs loaded with the ROS-sensitive fluorophore, H_2DCF-DA (10 μM), showed a significant increase in intracellular ROS concentration when exposed to 2.5 sec light pulses, in the presence of rr-P3HT. Conversely, the presence of the ROS scavenger, catalase (500 U/mL), strongly reduced the increase in H_2DCF-DA fluorescence. *** indicate $p < 0.001$. B. ECFCs stimulated with 20 sec light pulses, exhibited a similar ROS signal in the presence of rr-P3HT, which was significantly reduced in the presence of catalase. *** indicate $p < 0.001$. C. Ca^{2+} signal induced by 2.5 sec light pulse of optical stimulation of ECFCs cultured on rr-P3HT in the absence of ROS scavengers. D. The Ca^{2+} response to 2.5 sec long light pulses was significantly reduced by scavenging H_2O_2 production with catalase (500 U/mL). Washout of the scavenger resulted in a rebound and transient increase in $[Ca^{2+}]_i$. E. Dithiothreitol (DTT; 5 mM), a thiol-specific reducing compound, strongly reduced the Ca^{2+} response elicited by 2.5 sec long optical stimulation. F. Mean±SEM of the amplitude of light-induced Ca^{2+} signals in ECFCs plated on rr-P3HT under the designated treatments, i.e., in the presence of catalase, DTT, capsazepine (CAPZ), SB-366,791 (SB) or upon gene silencing of TRPV1 (siTRPV1). **** indicate $p < 0.0001$.

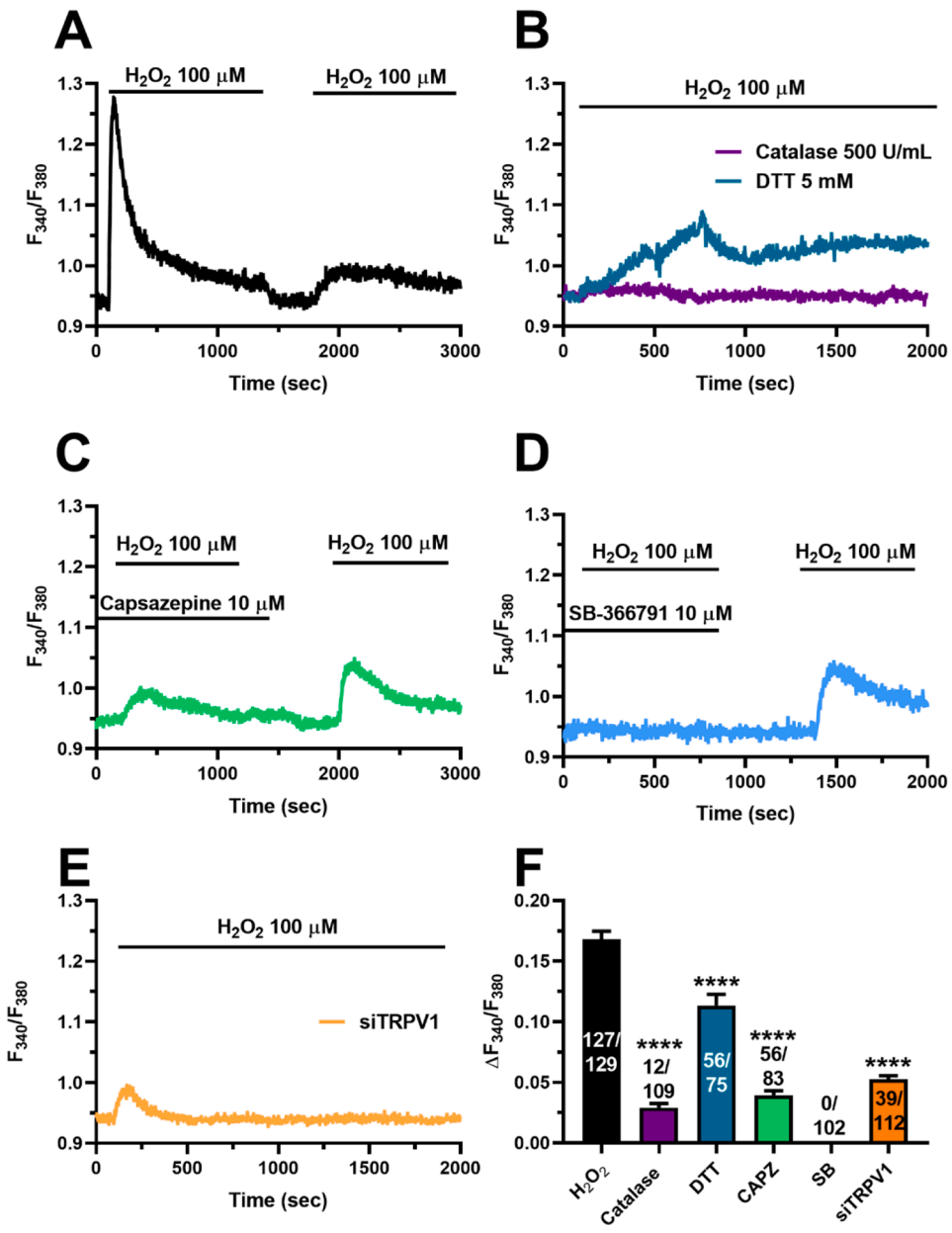

Fig. 7. H_2O_2 triggers TRPV1-dependent intracellular Ca^{2+} signals in ECFCs. A. H_2O_2 (100 μM) induced a biphasic increase in $[Ca^{2+}]_i$, characterized by an intermediate plateau phase which decayed to the baseline level with the washout of the agonist. B. The Ca^{2+} response to H_2O_2 (100 μM) was significantly inhibited by the scavenger catalase (500 U/ml) and by DTT (5 mM). C. The selective TRPV1 antagonist, capsazepine (10 μM, 30 min), strongly reduced H_2O_2-induced intracellular Ca^{2+} signals. A further stimulation with H_2O_2 (100 μM) evoked a prompted increase in $[Ca^{2+}]_i$ after the washout of the inhibitor. D. SB-366,791 (10 μM, 30 min), another specific TRPV1 inhibitor, completely abrogated H_2O_2-evoked Ca^{2+} signals in ECFCs. H_2O_2 was administered at 100 μM. E. Genetic silencing of TRPV1 expression with the specific siTRPV1 also impaired H_2O_2-induced intracellular Ca^{2+} signals in ECFCs. H_2O_2 was administered at 100 μM. F. Mean ± SEM of the amplitude of H_2O_2-induced Ca^{2+} signals under the designated treatments. **** indicate $p < 0.0001$.

[31]. To assess this issue, we first cultured ECFCs on a photoresist substrate (MicroPosit S1813), i.e., a fully electrically inert nanomaterial. Optical stimulation induced a Ca^{2+} response also under these conditions (Figure S5A). However, the percentage of responding cells (Figure S5B) was significantly ($p < 0.05$) lower, while the latency of the Ca^{2+} response (Figure S5C) was significantly ($p < 0.05$) longer, as compared to the Ca^{2+} signal recorded from ECFCs cultured on rr-P3HT thin films. Furthermore, the amplitude (Figure S5D) and duration (Figure S5A) of the Ca^{2+} response to optical excitation of S1813 were remarkably lower as compared to the increase in $[Ca^{2+}]_i$ evoked by light in the presence of rr-P3HT. Indeed, the Ca^{2+} response recorded in the absence of light-induced electrochemical reactions consisted in a transient elevation in $[Ca^{2+}]_i$ that rapidly recovered to the baseline (Figure S5A).

Therefore, we next investigated ROS involvement in the onset of the long lasting Ca^{2+} response to light in circulating ECFCs plated on rr-P3HT thin films. ECFCs loaded with the ROS-sensitive fluorophore, H_2DCF-DA (10 μM), exhibited a significant ROS signal when exposed to 2.5 sec (Fig. 6A) and 20 sec (Fig. 6B) light pulses only in the presence, but not in the absence, of rr-P3HT. Considering that the main ROS produced by optical stimulation of rr-P3HT thin films is hydrogen peroxide (H_2O_2) [24, 25, 62], we repeated the intracellular ROS measurement in the presence of the H_2O_2 scavenger, catalase (500 U/mL). As expected, there was not a significant increase in H_2DCF-DA fluorescence under these conditions (Fig. 6A and Fig. 6B) [56, 63]. In accord with this observation, scavenging H_2O_2 production with catalase (500 U/mL) significantly ($p < 0.0001$) reduced the Ca^{2+} response evoked in ECFCs by optical stimulation of rr-P3HT thin films (Fig. 6C and Fig. 6D). Washout of catalase from the bathing solution resulted in a rebound increase in $[Ca^{2+}]_i$ that rapidly declined to the baseline (Fig. 6D). Furthermore, dithiothreitol (DTT) (5 mM) (Fig. 6E), a thiol-specific reducing compound that is largely employed to reverse H_2O_2-mediated signaling [56, 64, 65], potently inhibited light-induced intracellular Ca^{2+} signals (Fig. 6E). The statistical analysis of these data has been shown in Fig. 6F. These observations strongly suggest that H_2O_2 is crucial to the onset of the Ca^{2+} response to polymer-mediated optical excitation of rr-P3HT thin films.

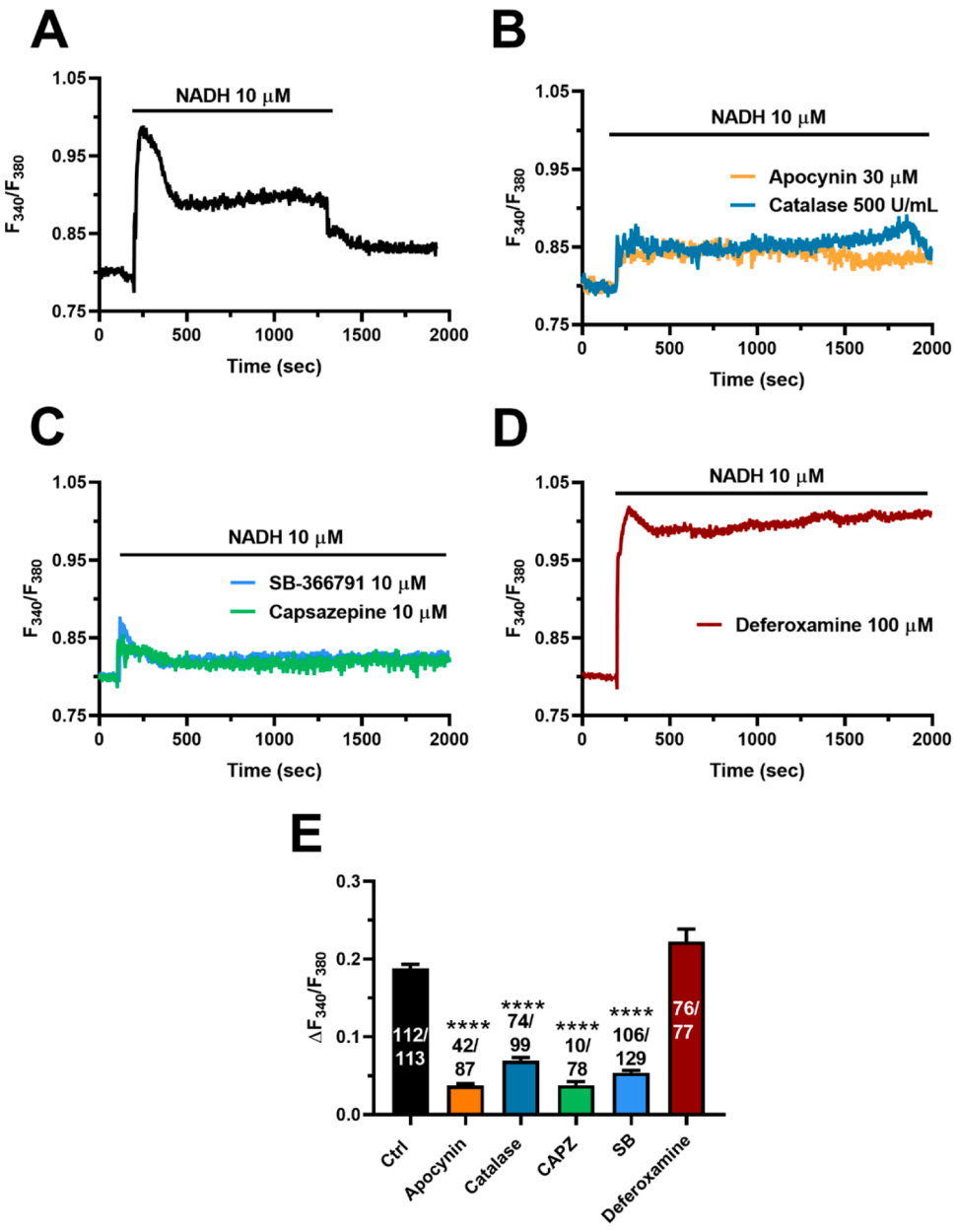

Fig. 8. NOX-dependent H_2O_2 production induced TRPV1-dependent intracellular Ca^{2+} signals in ECFCs. A. NADH (10 μM) evoked a biphasic increase in $[Ca^{2+}]_i$, characterized by an initial peak followed by an intermediate plateau phase, which decayed to the baseline with the washout of the molecule. B. NADH-evoked Ca^{2+} signals were significantly inhibited by catalase (500 U/ml) and by pre-treating the cells with apocynin (30 μM, 5 min), a selective NOX inhibitor. NADH was administered at 10 μM. C. NADH-induced increase in $[Ca^{2+}]_i$ was strongly reduced by inhibiting TRPV1 with either capsazepine (10 μM, 30 min) or SB-366,791 (10 μM, 30 min). NADH was administered at 10 μM. D. Deferoxamine (100 μM), which prevents the Fenton reaction by chelating Fe^{3+} and thus interferes with the subsequent lipid peroxidation, did not reduce the Ca^{2+} response to NADH (10 μM). E. Mean ± SEM of the amplitude of NADH-induced Ca^{2+} signals under the designated treatments, i.e., apocynin, catalase, capsazepine (CAPZ), SB-366,791 (SB), and deferoxamine. **** indicate $p<0.0001$.

3.6. H_2O_2 activates TRPV1-mediated intracellular Ca^{2+} signals in ECFCs

In order to confirm the signaling role of ROS in polymer-mediated Ca^{2+} response to photoexcitation, we directly challenged ECFCs with H_2O_2. As previously reported for capsaicin, H_2O_2 (100 μM) evoked a fast Ca^{2+} transient in 108 out of 363 cells (30%) and a biphasic Ca^{2+} signal in the remaining 232 cells (64%) (Fig. 7A). Similar to optical excitation, H_2O_2-induced Ca^{2+} signals were significantly ($p<0.05$) inhibited by catalase (500 U/ml) and by DTT (5 mM) (Fig. 7B). Furthermore, the Ca^{2+} response to H_2O_2 (100 μM) was significantly ($p < 0.05$) reduced by blocking TRPV1 with either capsazepine (10 μM, 30 min) (Fig. 7C) or by SB-366,791 (10 μM, 30 min) (Fig. 7D). Finally, genetic disruption of TRPV1 protein expression through the specific siTRPV1 also impaired H_2O_2-induced increase in $[Ca^{2+}]_i$ (Fig. 7E). The statistical analysis of these data has been summarized in Fig. 7F.

Exogenous administration of nicotinamide adenine dinucleotide phosphate (NADH) represents an additional strategy to investigate H_2O_2 signaling in endothelial cells [66, 67]. NADH is converted by the membrane-bound enzyme, NAD(P)H-oxidase (NOX), into superoxide radical (O_2^-), which may be then dismutated to H_2O_2 either spontaneously or by superoxide dismutase [68]. NADH (10 μM) evoked an increase in $[Ca^{2+}]_i$ that was inhibited by pre-treating the cells with apocynin (30 μM, 5 min) (Fig. 8A and Fig. 8B), a selective NOX inhibitor [67]. Furthermore, the Ca^{2+} response to NADH (10 μM) was significantly ($p < 0.0001$) reduced by catalase (500 U/ml) (Fig. 8A and Fig. 8B). This observation confirms that H_2O_2 generation is required by NADH to induce intracellular Ca^{2+} signals in ECFCs. Furthermore, NADH-evoked increase in $[Ca^{2+}]_i$ was dramatically attenuated by blocking TRPV1 with either capsazepine (10 μM, 30 min) (Fig. 8C) or by SB-366,791 (10 μM, 30 min) (Fig. 8C). In the presence of iron (Fe^{2+}), the Fenton reaction could degrade H_2O_2 into the hydroxyl radical, $OH^{\bullet}$ [68], which may also result in Ca^{2+} signaling via lipid peroxidation [67, 69]. However, the Ca^{2+} response to NADH (10 μM) was not affected by deferoxamine (100 μM) (Fig. 8D), which prevents the Fenton reaction by chelating ferric iron (Fe^{3+}) [67, 69]. The statistical analysis of these data has been summarized in Fig. 8E. In aggregate, these findings endorse the view that H_2O_2 produced upon optical excitation of rr-P3HT may induce intracellular Ca^{2+} signals by activating TRPV1 in circulating ECFCs.

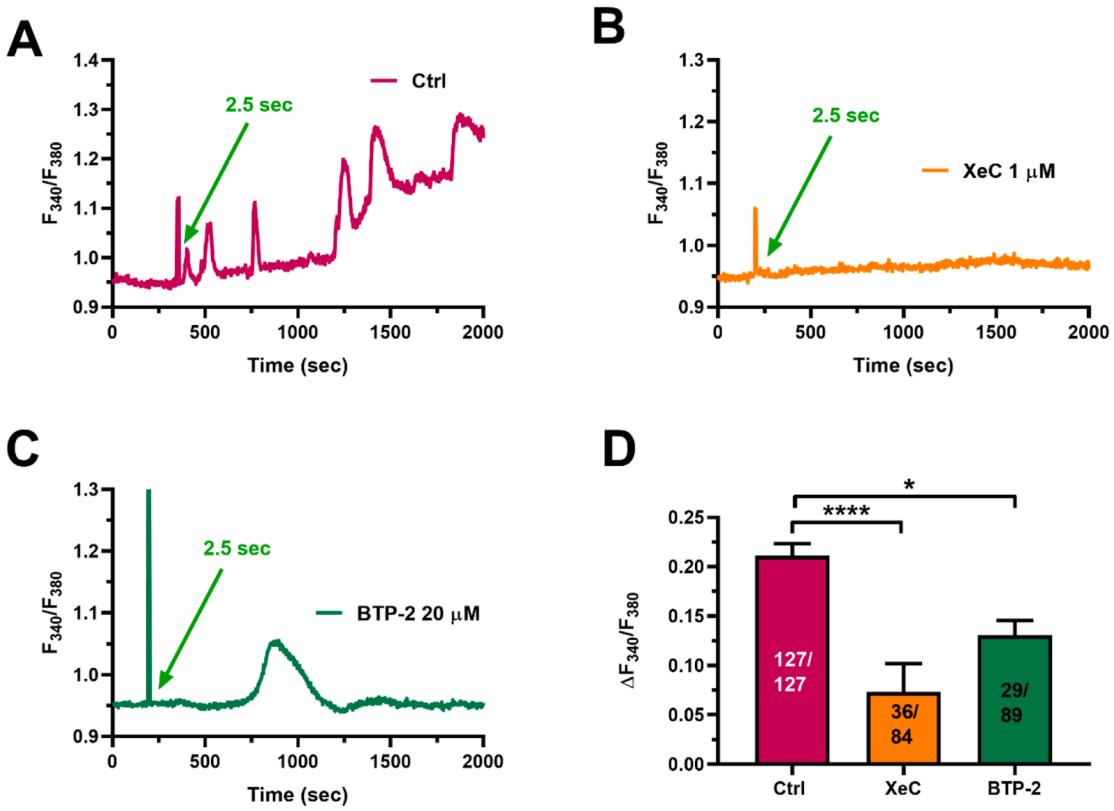

Fig. 9. Inositol-1,4,5-trisphosphate ($InsP_3$) receptors ($InsP_3Rs$) and store-operated Ca^{2+} entry (SOCE) were involved in the Ca^{2+} response evoked by polymer-mediated optical excitation. A. 2.5 sec light pulse induced a robust increase in $[Ca^{2+}]_i$ in ECFCs plated on rr-P3HT thin films under control conditions. B. Light-induced Ca^{2+} signal was inhibited by blocking $InsP_3Rs$ with Xestospongin C (XeC; 1 μM, 10 min). C. Pre-treatment of cells with the selective SOCE inhibitor, BTP-2 (20 μM, 30 min), significantly reduced and shortened the Ca^{2+} response to optical stimulation. D. Mean ± SEM of the amplitude of light-induced Ca^{2+} signals under the designated treatments. **** indicate $p<0.0001$ and * indicates $p<0.05$.

3.7. The role of inositol-1,4,5-trisphosphate ($InsP_3$) receptors ($InsP_3Rs$) and store-operated Ca^{2+} entry (SOCE) in the Ca^{2+} response evoked by polymer-mediated optical excitation

The intracellular Ca^{2+} oscillations that arose in a significant fraction of ECFCs exposed to light stimuli in the presence of rr-P3HT resemble $InsP_3$-induced intracellular Ca^{2+} spikes from the endoplasmic reticulum (ER) [52, 70, 71], which represents the largest endogenous Ca^{2+} store in vascular endothelial cells and ECFCs [72]. In addition, $InsP_3Rs$ may also contribute to trigger slowly rising Ca^{2+} signals in response to extracellular stimulation [73–75]. Notably, the pharmacological blockade of $InsP_3Rs$ with the selective inhibitor, XeC (1 μM, 10 min), prevented light-induced Ca^{2+} signals in the majority of ECFCs (100%, $n = 127$, and 42.8%, $n = 84$, in the absence and presence of XeC, respectively. Inspection of the Ca^{2+} tracings showed that, as compared to control cells (Fig. 9A), the amplitude of the maximum variation in $[Ca^{2+}]_i$ was significantly ($p < 0.0001$) lower in the presence of XeC (Fig. 9B and Fig. 9D). $InsP_3$-induced ER Ca^{2+} mobilization, in turn, results in a massive depletion of ER Ca^{2+} levels, which activates a Ca^{2+}-entry pathway known as store-operated Ca^{2+} entry (SOCE) [76]. SOCE maintains long-lasting intracellular Ca^{2+} signals evoked by extracellular stimuli in vascular endothelial cells and ECFCs [52, 77]. Of note, blocking SOCE with the pyrazole-derivative BTP-2 (20 μM, 30 min) [77–79], reduced the percentage of ECFCs displaying a detectable Ca^{2+} response to light stimuli to 32.6% ($n = 89$). In these cells, BTP-2 converted the long-lasting increase in $[Ca^{2+}]_i$ evoked by optical excitation in a transient Ca^{2+} signal (Fig. 9C), whose amplitude was significantly ($p < 0.5$) lower than the amplitude of the plateau phase recorded in control cells (Fig. 9D). Collectively, therefore, these data suggest that TRPV1-mediated extracellular Ca^{2+} entry may be amplified into a long-lasting elevation in $[Ca^{2+}]_i$ through the recruitment of $InsP_3Rs$ followed by SOCE activation, as more widely described in Section 4.4.

4. Discussion

Optical modulation through exogenous photoactive materials is emerging as a powerful, geneless, and minimally invasive tool able to control cellular activity and to rescue defective signaling pathways with unprecedented spatial resolution, potentially at the sub-cell organelles level, and with highly versatile temporal patterns. In this context, semiconducting conjugated polymers, such as rr-P3HT, have been proven to be highly reliable materials, able to effectively control cell functionality in several biomedical applications [10–13]. Nevertheless, the biological signal(s) whereby photostimulation of P3HT, taken as a prototypical photoactive material, drive(s) cellular behaviours that are relevant for the recovery of specific lost functions are yet to be fully unraveled [10, 12]. Herein, we provided the first evidence that the non-selective cation channel, TRPV1, is activated by rr-P3HT-mediated optical excitation to induce an increase in $[Ca^{2+}]_i$ in circulating ECFCs, that represent the most suitable cellular substrate to induce therapeutic angiogenesis of ischemic tissues [2–4]. We further show that H_2O_2, which is produced at the interface between the rr-P3HT thin film and the cellular membrane [10, 80], is the main responsible for light-induced TRPV1 activation and extracellular Ca^{2+} entry. These findings contribute to unravel the molecular mechanisms whereby optical excitation of rr-P3HT could stimulate circulating ECFCs to effect vascular regrowth in ischemic tissues.

4.1. Optical excitation of rr-P3HT thin films causes an increase in $[Ca^{2+}]_i$ in circulating ECFCs

Pro-angiogenic stimuli, such as vascular endothelial growth factor (VEGF) [45], stromal derived factor-1α (SDF-1α), and the human amniotic fluid stem cell secretome [53], evoke different intracellular Ca^{2+} waveforms, such as intracellular Ca^{2+} oscillations and biphasic Ca^{2+} elevations in circulating ECFCs. Furthermore, a recent report from our group demonstrated that optical excitation (light power density 0.4 mW/mm^2) of rr-P3HT thin films stimulated ECFCs to proliferate and assemble into capillary-like networks [31]. The pro-angiogenic effect of optical excitation was abrogated by pre-treating the cells with BAPTA-AM, a membrane-permeable buffer of intracellular Ca^{2+} levels [31]. This observation hinted at a crucial role played by Ca^{2+} signaling in polymer-mediated photoexcitation of ECFCs' pro-angiogenic activity [9, 11]. We now confirmed this hypothesis by showing that a similar protocol of photostimulation (i.e., light power density 0.6 mW/mm^2) of ECFCs cultured on rr-P3HT thin films induced an increase in $[Ca^{2+}]_i$ that could adopt multiple patterns. Around half of ECFCs subjected to 2.5 sec light pulses displayed a delayed, slow increase in $[Ca^{2+}]_i$. The remaining half of ECFCs presented intracellular Ca^{2+} oscillations, consisting of repeated Ca^{2+} transients overlapping the slowly developing $[Ca^{2+}]_i$ rise. Interestingly, pro-angiogenic cues, which stimulate long-lasting processes, such as endothelial cell proliferation, migration, and tube formation, usually evoke quite heterogeneous intracellular Ca^{2+} signatures [49–52]. For instance, VEGF-induced intracellular Ca^{2+} oscillations stimulate ECFC proliferation and in vitro tubulogenesis through the nuclear translocation of the Ca^{2+}-sensitive transcription factor, nuclear factor-κB (NF-κB) [45, 52], as also observed in circulating ECFCs challenged with the human amniotic fluid stem cell secretome [53, 81]. On the other hand, SDF-1α was found to promote ECFC migration, both in vitro and in vivo, by eliciting biphasic Ca^{2+} signals in ECFCs that recruited extracellular signal-regulated kinase (ERK) and phosphoinositide 3-kinases (PI3K)/Akt [8]. Likewise, early work revealed that insulin-like growth factor 2 could induce postnatal vasculogenesis by eliciting a non-oscillatory Ca^{2+} signal in circulating ECFCs [82]. A recent investigation from our group revealed that rr-P3HT-mediated optical excitation of ECFCs stimulated proliferation and tubulogenesis through the Ca^{2+}-dependent recruitment of NF-κB [31]. Although the photoexcitation protocols employed in the two studies are slightly different (chronic exposure to pulsed illumination in [31], single light pulses here), these findings suggest that light-induced intracellular Ca^{2+} oscillations could preferentially induce ECFC to proliferate and assembly into capillary-like structure, whereas the non-oscillatory elevation in $[Ca^{2+}]_i$ could rather be coupled to the Ca^{2+}-dependent motility machinery. This hypothesis is further corroborated by the recent evidence that VEGF may trigger distinct functional responses in vascular endothelial cells depending on the pattern of the Ca^{2+} response, whereas intracellular Ca^{2+} oscillations and biphasic Ca^{2+} signals selectively lead to proliferation and migration, respectively [51].

Photoexcitation of ECFCs cultured on bare glass substrate did not reliably increase the $[Ca^{2+}]_i$. In agreement with this and previous observations [31], photobiomodulation mediated by endogenous chromophores is able to elicit endothelial signaling only at wavelengths longer than 625 nm [83]. This is, therefore, the first evidence that optical stimulation of rr-P3HT thin layers by visible light induces intracellular Ca^{2+} signals in a cellular model with a potentially high therapeutic relevance [3]. Furthermore, our observations are consistent with previous reports showing that photocatalytic activity of rr-P3HT nanoparticles internalized within the cytoplasm caused an increase in $[Ca^{2+}]_i$ in HEK-293 cells [24], which was not due to physiological signaling and not to unwanted dismantling of the Ca^{2+} handling machinery [84].

4.2. Extracellular Ca^{2+} entry through TRPV1 drives the increase in $[Ca^{2+}]_i$ evoked by optical excitation of rr-P3HT thin films

Recent work from our group demonstrated that photoexcitation of circulating ECFCs growing on rr-P3HT thin films lead to the activation of the non-selective cation channel TRPV1 on the plasma membrane, thereby inducing ECFC depolarization [31]. TRPV1 is significantly more permeable to Ca^{2+} over Na^+ and displays a permeability ratio, P_{Ca}/P_{Na}, around 5 [9, 28]. TRPV1 was therefore the most likely candidate to trigger the Ca^{2+} response to photoexcitation. In agreement with this hypothesis, we first found that extracellular Ca^{2+} entry was strictly required both to trigger the Ca^{2+} signal and to maintain the increase in $[Ca^{2+}]_i$ observed in all ECFCs subjected to light stimulation. The following pieces of evidence demonstrate that TRPV1 provides the main pathway to sustain the influx of Ca^{2+} evoked by photoexcitation. First, TRPV1 protein was abundantly expressed in circulating ECFCs, as previously observed in umbilical cord blood-derived ECFCs [85]. The size of TRPV1 protein in ECFCs is within the same range as that described in peripheral nociceptors, i.e., 100 kDa [28], whereas, in other cell types, it can undergo post-translational modifications that induce significant alterations in the molecular weight (≈75 kDa) [86, 87]. Second, capsaicin, a selective TRPV1 agonist [28, 56, 57], caused an increase in $[Ca^{2+}]_i$ that was dampened by two structurally distinct TRPV1 blockers, such as capsazepine and SB-366,791 [9, 27, 56, 57, 60, 61]. Third, the genetic deletion of TRPV1 protein with a selective siTRPV1 strongly inhibited capsaicin-induced intracellular Ca^{2+} signals. The efficacy of this construct to downregulate extracellular Ca^{2+} entry through TRPV1 has already been proved in metastatic colorectal cancer cells [57]. Fourth, the pharmacological (with capsazepine or SB-366,791) and genetic (with the selective siTRPV1) blockade of TRPV1 significantly inhibited light-induced intracellular Ca^{2+} signals in ECFCs cultured on rr-P3HT thin films. These findings provide the first evidence that TRPV1 may effectively translate optical excitation of a photosensitive organic semiconductor, such as rr-P3HT, in an increase in $[Ca^{2+}]_i$. It is worth pointing out that TRPV1 is emerging as the ideal target of other nanotechnological strategies. For instance, TRPV1 can also be activated by magnetic nanoparticles exposed to alternating magnetic fields and thereby elicit neuronal activity within the ventral tegmental area in mouse brain [88]. Furthermore, near infrared light-dependent stimulation of gold nanorods restored the visual function in a mouse model of degenerative blindness upon viral-mediated delivery of TRPV1 in retinal cones [89]. Therefore, TRPV1 activation could represent the molecular mechanism onto which multiple nanotechnological solutions converge to rescue defective Ca^{2+} signaling, e.g., in neurons, or to stimulate pro-angiogenic Ca^{2+} signals, e.g., in circulating ECFCs.

4.3. The primary role of ROS in TRPV1 activation upon optical excitation of rr-P3HT thin films

TRPV1 is a polymodal channel that may effectively integrate the two main biologically relevant signals generated by the photocatalytic activity of rr-P3HT thin films [9, 11, 27, 28, 56], i.e., the local increase in temperature and in H_2O_2 levels at the interface between the substrate and the cell membrane [14, 24, 25, 62]. TRPV1 may indeed serve as a sensor for noxious heat (>41 °C) [28] and is also directly activated by H_2O_2 [56, 64]. Elucidation of the phototransduction mechanisms showed that ROS, but not heat, were responsible for light-induced ECFC proliferation and in vitro tubulogenesis in the presence of rr-P3HT thin films [31]. This study further highlights the interplay among photoelectrochemical activity, ROS generation, TRPV1 activation and modulation of $[Ca^{2+}]_i$. In accord, optical excitation of a photoresist substrate that does not undergo the photoelectrochemical reaction, did not reliably increase the $[Ca^{2+}]_i$ in circulating ECFCs. Furthermore, this Ca^{2+} signal only exhibited a transient duration, presented a longer latency and was remarkably lower as compared to rr-P3HT-mediated Ca^{2+} responses. This finding is consistent with our previous report that the

global increase in temperature upon light exposure does not reach the thermal threshold required for TRPV1 activation by heat (≈38 °C vs. 41 °C) [27]. We cannot rule out the possibility that the local elevation in temperature at the interface between the photoresist nanomaterial and some ECFCs may activate TRPV1; however, this thermal signal does not suffice to induce the long-lasting increase in $[Ca^{2+}]_i$ that regularly arises upon optical excitation of rr-P3HT. Second, a robust increase in intracellular ROS levels occurs in ECFCs growing on rr-P3HT thin films, but not on glass substrates, and subjected to 2.5 sec- and 20 sec-long light pulses. Although H_2DCF-DA does not selectively detect H_2O_2 [90], the increase in ROS production induced by photoexcitation of rr-P3HT was abrogated by scavenging H_2O_2 with catalase [56, 63]. In agreement with these observations, the increase in $[Ca^{2+}]_i$ induced by polymer-mediated optical excitation was abrogated by catalase and significantly reduced by DTT, which is commonly employed to reverse H_2O_2-dependent TRPV1 activation by reducing the thiol groups involved in channel opening [56, 64, 65].

To further corroborate the gating role played by H_2O_2 in the TRPV1-mediated Ca^{2+} response to photoexcitation, we adopted two different strategies. Acute H_2O_2 exposure caused an increase in $[Ca^{2+}]_i$ that was abrogated by catalase and strongly decreased by DTT. Furthermore, H_2O_2-induced intracellular Ca^{2+} signals were reversibly inhibited by the pharmacological (with capsazepine or SB-366791) and genetic (with the selective siTRPV1) deletion of TRPV1. H_2O_2 was known to elevate the $[Ca^{2+}]_i$ [91–93] and to activate TRPV1-mediated transmembrane currents [56] in vascular endothelial cells. However, this is the first evidence that TRPV1 contributes to H_2O_2-induced intracellular Ca^{2+} signals in the endothelial lineage. In a next set of experiments, circulating ECFCs were challenged with NADH, the substrate of NOX enzymes, which catalyze the transfer of an electron from NAD(P)H to molecular oxygen (O_2), thereby generating the $O_2^{\cdot -}$ [67, 94]. $O_2^{\cdot -}$ can then be dismutated into H_2O_2, which, in the presence of Fe^{2+}, can in turn be degraded to $OH^{\bullet}$ through the Fenton reaction [67, 94]. A recent report identified NOX4 as the major NOX isoform expressed in ECFCs [95]. Herein, we found that NADH induced an increase in $[Ca^{2+}]_i$ that was significantly attenuated by blocking NOX activity with apocynin and scavenging extracellular H_2O_2 with catalase. In agreement with these observations, the Ca^{2+} response to NADH was hindered by blocking TRPV1 with either capsazepine or SB-366,791. Furthermore, preventing the Fenton reaction with deferoxamine enhanced, rather than decreasing, NADH-induced intracellular Ca^{2+} signals in ECFCs. This observation is consistent with the notion that $OH^{\bullet}$-induced peroxidation of membrane lipids may somehow inhibit TRPV1 activity in microvascular endothelial cells [96]. These findings, therefore, collectively hint at H_2O_2 as the biological signal gating TRPV1 in the plasma membrane of ECFCs upon optical excitation of rr-P3HT thin films. Since H_2O_2 is crucial to stimulate extracellular Ca^{2+} entry in photoexcited ECFCs, we cannot rule out the possibility that other ROS-sensitive TRP channels, such as TRPM Melastatin 2 (TRPM2) and TRP Ankyrin 1 (TRPA1) [94, 97]. However, TRPA1 is seemingly expressed only in brain microvascular endothelial cells, in which Ca^{2+} entry is gated by lipid peroxidation [67, 98], thereby suggesting that this TRP isoform is not involved in rr-P3HT-mediated increase in $[Ca^{2+}]_i$ in ECFCs. TRPM2, in turn, has been shown to trigger ROS-sensitive endothelial Ca^{2+} signals in multiple vascular beds [99]. TRPM2 activation is, however, secondary to H_2O_2-induced mitochondrial production of ADP ribose and may be sustained over time by the accompanying binding of Ca^{2+} [97]; therefore, TRPM2 is unlikely to be the primary target of H_2O_2 on the plasma membrane upon its diffusion across the phospholipid bilayer. Nevertheless, investigations are underway in our group to assess whether TRPA1 and TRPM2 somehow contribute to the residual Ca^{2+} response arising in ECFCs following the pharmacological (with capsazepine and SB-366,791) and genetic (with the specific siTRPV1) blockade of TRPV1.

4.4. Putting all the pieces together: the role of $InsP_3Rs$ and SOCE

The complex increase in $[Ca^{2+}]_i$ evoked by visible light in a remarkable fraction (≈50%) of ECFCs growing on rr-P3HT thin films encompasses fast Ca^{2+} transients that could overlap the slowly developing rise in $[Ca^{2+}]_i$. These repetitive Ca^{2+} oscillations are strongly reminiscent of the $InsP_3$-induced Ca^{2+} release events that are often elicited by growth factors in both vascular endothelial cells [50, 51] and ECFCs [45, 53]. This observation led us to speculate about $InsP_3R$ engagement by TRPV1. Indeed, extracellular Ca^{2+} entry across the plasma membrane may recruit ER-embedded $InsP_3Rs$ through the mechanism of Ca^{2+}-induced Ca^{2+} release (CICR) in vascular endothelial cells [100, 101]. Furthermore, H_2O_2 may enhance $InsP_3R$ sensitivity to ambient $InsP_3$ concentration ($[InsP_3]$) and thereby mobilize ER Ca^{2+} [102], as also shown in endothelial cells from multiple vascular districts [92, 93]. ECFCs express all the three $InsP_3R$ subtypes ($InsP_3R1$–3), while they lack ryanodine receptors [55], which represent the canonical target for CICR [103]. Quite surprisingly, XeC, a selective blocker of $InsP_3Rs$, did not only abolish the intracellular Ca^{2+} oscillations; it also strongly dampened the global Ca^{2+} response evoked in ECFCs by the photoexcitation of rr-P3HT thin films. This unexpected finding led us to hypothesize the involvement of an additional Ca^{2+} entry pathway, i.e., SOCE, which is activated downstream of $InsP_3Rs$ [76]. SOCE is mediated by the physical interaction between STIM1, the sensor of ER Ca^{2+} concentration, and the Ca^{2+}-permeable channels, Orai1 and Transient Receptor Potential Canonical 1 (TRPC1) on the plasma membrane [76, 78]. SOCE develops over seconds to ten of seconds upon $InsP_3$-dependent depletion of the ER Ca^{2+} pool and sustains the long-lasting duration of the Ca^{2+} signals evoked in ECFCs by pro-angiogenic cues [8, 52, 55]. Of note, pre-treating the cells with BTP-2, a selective blocker of SOCE in ECFCs [8, 76], extended the latency, reduced the amplitude and strongly curtailed the duration of the Ca^{2+} response to optical excitation, which adopted a transient pattern.

These findings provide the first evidence that $InsP_3Rs$ and SOCE may participate to the phototransduction mechanisms whereby optical modulation of rr-P3HT thin films controls cellular activity (Fig. S6). Furthermore, this novel evidence permits to better understand how H_2O_2 and TRPV1 trigger the intracellular Ca^{2+} signals that drive light-induced ECFC proliferation and tube formation. H_2O_2 produced at the interface between rr-P3HT thin films and the extracellular solution may freely permeate through the plasma membrane [94] and oxidize the cysteine-thiol groups that are located in the cytosolic COOH- and NH_2-terminal tails of TRPV1 [64]. This in turn results in a kinetically slow increase in $[Ca^{2+}]_i$ that is likely to reflect the rate of H_2O_2 production and accumulation beneath the cytosolic membrane leaflet. The real-time measurement of light-induced increases in cytosolic H_2O_2 by using electrochemical probes is currently underway [104]. Extracellular Ca^{2+} entry through TRPV1 is strictly required to initiate the Ca^{2+} response, as no rise in $[Ca^{2+}]_i$ can be detected under $0Ca^{2+}$ conditions, when $InsP_3$-induced ER Ca^{2+} release may still occur. The subsequent influx of Ca^{2+} may in turn contribute to sensitize $InsP_3Rs$ to ambient $[InsP_3]$, a process that could also be directly promoted by H_2O_2 reaching the bulk cytosol [92, 93]. $InsP_3Rs$ contribute to support the slowly developing increase in $[Ca^{2+}]_i$ triggered by TRPV1 that culminates in SOCE activation when ER Ca^{2+} falls below the threshold required for the engagement of STIM1.

Notably, the unpredictable occurrence of ER Ca^{2+} spikes could reflect differences in ambient $[InsP_3]$ within different sub-regions of the same cell and/or among different ECFCs, which might therefore result in different sensitivities to $InsP_3$-induced Ca^{2+} release. In other words, upon TRPV1-mediated extracellular Ca^{2+} entry, some compartments of the ER could discharge in a less-synchronous manner (low ambient $[InsP_3]$) and contribute to the slowly rising Ca^{2+} signal. Other sub-regions of the ER could instead result in the well synchronized events of Ca^{2+} release that underlie fast Ca^{2+} spikes (high ambient $[InsP_3]$). This biphasic mode of $InsP_3R$ signaling depending upon ambient $[InsP_3]$

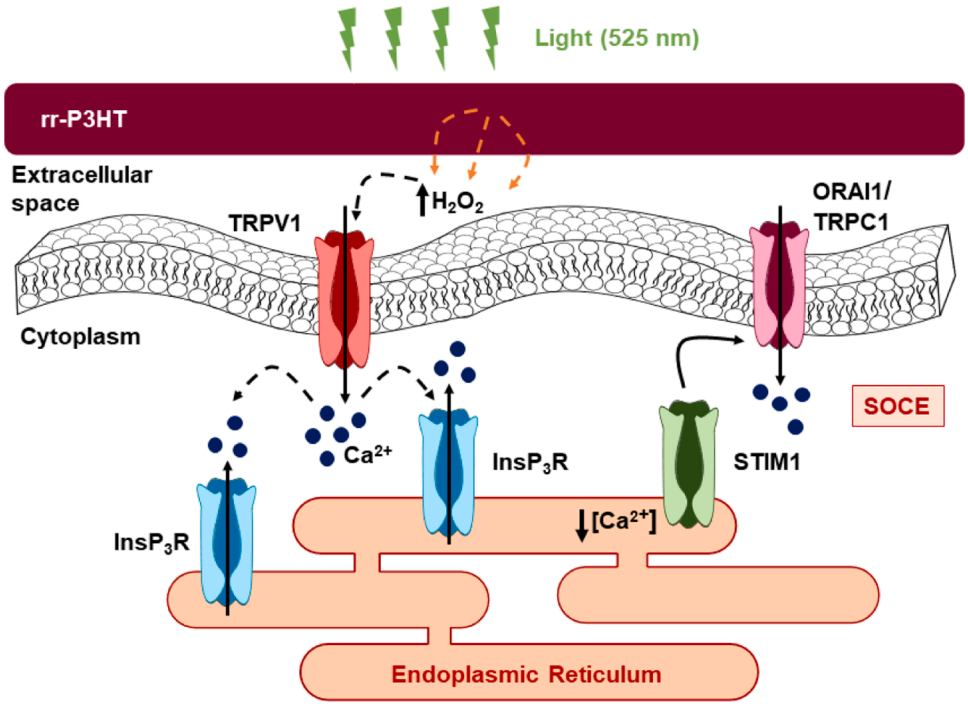

Fig. 10. Schematic representation of the molecular mechanisms leading to the Ca^{2+} response to visible excitation in circulating ECFCs plated on rr-P3HT thin films. Optical stimulation of ECFCs plated on rr-P3HT induced the production of H_2O_2 between the thin film and the cell membrane. H_2O_2 in turn, activates TRPV1, thereby leading to extracellular Ca^{2+} entry that can, in turn, promote the Ca^{2+}-dependent recruitment of $InsP_3Rs$ on ER membrane. The following release of intraluminal Ca^{2+} leads to a dramatic reduction in endoplasmic reticulum (ER) Ca^{2+} concentration ($[Ca^{2+}]_i$), which leads to the STIM1-dependent activation of SOCE through Orai1 and TRPC1 channels on the plasma membrane.

has been proposed to mediate the intracellular Ca^{2+} oscillations evoked in non-excitable cells [73, 75], including vascular endothelial cells [74], by the thiol oxidizing reagent, thimerosal. Alternately, intracellular Ca^{2+} oscillations could arise depending on whether H_2O_2 recruits phospholipase C (PLC) [105], the membrane receptor responsible for $InsP_3$ cleavage from phosphatidylinositol 4,5-bisphosphate [106], which could locally boost $InsP_3$ synthesis and induce fast events of ER Ca^{2+} release.

A feature of the Ca^{2+} response to optical excitation of rr-P3HT thin films that deserves to be addressed is that the latency of the signal increases while the percentage and frequency of oscillating cells decrease at longer light pulses. Excessive H_2O_2 levels could indirectly dampen endothelial $InsP_3Rs$ by depolarizing the mitochondrial membrane potential [107]. Therefore, upon exposure to light pulses longer than 2.5 sec, $InsP_3Rs$-mediated ER Ca^{2+} release could be somehow hindered by the larger H_2O_2 production, thereby delaying the slow increase in $[Ca^{2+}]_i$ evoked by TRPV1 and progressively lowering the probability that Ca^{2+} oscillations arise. The assessment of this hypothesis requires a quantitatively more precise measurement of ROS and H_2O_2 upon exposure to increasingly longer light stimuli and the evaluation of $InsP_3R$ inhibition by high H_2O_2 concentrations.

5. Conclusion

We have provided the first evidence that TRPV1 translates optical excitation of rr-P3HT thin films in a long lasting Ca^{2+} signal in a therapeutically relevant cell model, such as circulating ECFCs. This increase in $[Ca^{2+}]_i$ in turn mediate ECFCs' angiogenic activity in vitro [31] and could thereby favor therapeutic angiogenesis in vivo, although this latter hypothesis remains to be experimentally probed. H_2O_2 plays a central role in TRPV1 activation by light, as confirmed by multiple approaches, whereas $InsP_3Rs$ and SOCE amplify TRPV1-mediated extracellular Ca^{2+} entry into a sustained Ca^{2+} signal (Fig. 10). The proof-of-concept that photostimulation of rr-P3HT induces TRPV1-mediated Ca^{2+} signals in a therapeutically relevant cell model will broaden the application of organic semiconductors to the treatment of diseases associated to defective Ca^{2+} dynamics, including heart failure [108], neurodegenerative [109, 110] and muscular [111] disorders. Furthermore, optical stimulation of rr-P3HT thin films could provide a reliable strategy to mitigate Ca^{2+}-dependent endothelial dysfunction in a plethora of cardiovascular disorders [112, 113], including those associated to SARS-CoV-2 [114].

6. Funding

This research was supported by: EU Horizon 2020 FETOPEN-2018–2020 Programme 'LION—HEARTED', grant agreement n. 828,984 (F.M., M.R.A., F.L); European Research Council (ERC) under the European Union's Horizon 2020 research and innovation program 'LINCE', grant agreement n. 803,621 (M.R.A); Italian Ministry of Education, University and Research (MIUR): Dipartimenti di Eccellenza Program (2018–2022) - Dept. of Biology and Biotechnology "L. Spallanzani", University of Pavia (F.M.), Fondo Ricerca Giovani from the University of Pavia (F.M.), and by Fondazione "Ca' della Paglia" (S.N.).

CRediT authorship contribution statement

Sharon Negri: Conceptualization, Data curation, Formal analysis, Investigation, Writing – review & editing. **Pawan Faris:** Data curation, Formal analysis, Investigation. **Gabriele Tullii:** Data curation, Formal analysis, Investigation. **Mauro Vismara:** Data curation, Formal analysis, Investigation. **Alessandro F. Pellegata:** Data curation, Formal analysis, Investigation. **Francesco Lodola:** Data curation, Formal analysis, Investigation. **Gianni Guidetti:** Data curation, Formal analysis, Investigation. **Vittorio Rosti:** Investigation, Methodology. **Maria Rosa Antognazza:** Conceptualization, Funding acquisition, Investigation, Project administration, Resources, Supervision, Validation, Writing – review & editing. **Francesco Moccia:** Conceptualization, Funding acquisition, Investigation, Project administration, Resources, Supervision, Validation, Writing – original draft.

Declaration of Competing Interest

Declarations of interests: none.

References

[1] R.J. Medina, C.L. Barber, F. Sabatier, F. Dignat-George, J.M. Melero-Martin, K. Khosrotehrani, O. Ohneda, A.M. Randi, J.K.Y. Chan, T. Yamaguchi, V.W. M. Van Hinsbergh, M.C. Yoder, A.W. Stitt, Endothelial progenitors: a consensus statement on nomenclature, Stem Cells Transl. Med. 6 (2017) 1316–1320.

[2] C.L. O'Neill, K.J. McLoughlin, S.E.J. Chambers, J. Guduric-Fuchs, A.W. Stitt, R. J. Medina, The Vasoreparative Potential of endothelial colony forming cells: a journey through pre-clinical studies, Front. Med. (Lausanne) 5 (2018) 273.

[3] P. Faris, S. Negri, A. Perna, V. Rosti, G. Guerra, F. Moccia, Therapeutic potential of endothelial colony-forming cells in ischemic disease: strategies to improve their regenerative efficacy, Int. J. Mol. Sci. 21 (2020).

[4] K.E. Paschalaki, A.M. Randi, Recent advances in endothelial colony forming cells toward their use in clinical translation, Front. Med. (Lausanne) 5 (2018) 295.

[5] D. Tasev, P. Koolwijk, V.W. van Hinsbergh, Therapeutic potential of human-derived endothelial colony-forming cells in animal models, Tissue Eng. Part B Rev. 22 (2016) 371–382.

[6] F. Moccia, R. Berra-Romani, V. Rosti, Manipulating intracellular Ca2+ signals to stimulate therapeutic angiogenesis in cardiovascular disorders, Curr. Pharm. Biotechnol. 19 (2018) 686–699.

[7] S.C. Heo, Y.W. Kwon, I.H. Jang, G.O. Jeong, J.W. Yoon, C.D. Kim, S.M. Kwon, Y. S. Bae, J.H. Kim, WKYMVm-induced activation of formyl peptide receptor 2 stimulates ischemic neovasculogenesis by promoting homing of endothelial colony-forming cells, Stem Cells 32 (2014) 779–790.

[8] E. Zuccolo, C. Di Buduo, F. Lodola, S. Orecchioni, G. Scarpellino, D.A. Kheder, V. Poletto, G. Guerra, F. Bertolini, A. Balduini, V. Rosti, F. Moccia, Stromal cell-derived factor-1alpha promotes endothelial colony-forming cell migration through the Ca(2+)-dependent activation of the extracellular signal-regulated kinase 1/2 and phosphoinositide 3-kinase/AKT pathways, Stem Cells Dev. 27 (2018) 23–34.

[9] S. Negri, P. Faris, V. Rosti, M.R. Antognazza, F. Lodola, F. Moccia, Endothelial TRPV1 as an emerging molecular target to promote therapeutic angiogenesis, Cells 9 (2020).

[10] M.R. Antognazza, I. Abdel Aziz, F. Lodola, Use of exogenous and endogenous photomediators as efficient ROS modulation tools: results and perspectives for therapeutic purposes, Oxid. Med. Cell. Longev. (2019), 2867516, 2019.

[11] F. Moccia, M.R. Antognazza, F. Lodola, Towards novel geneless approaches for therapeutic angiogenesis, Front. Physiol. 11 (2020), 616189.

[12] F. Di Maria, F. Lodola, E. Zucchetti, F. Benfenati, G. Lanzani, The evolution of artificial light actuators in living systems: from planar to nanostructured interfaces, Chem. Soc. Rev. 47 (2018) 4757–4780.

[13] M.R. Antognazza, N. Martino, D. Ghezzi, P. Feyen, E. Colombo, D. Endeman, F. Benfenati, G. Lanzani, Shedding light on living cells, Advanced materials, 27 (2015) 7662–7669.

[14] J. Hopkins, R. Travaglini, A. Lauto, T. Cramer, B. Fraboni, J. Seidel, D. Mawad, Photoactive organic substrates for cell stimulation: progress and perspectives, Adv. Mater. Technol 4 (2019) 10.

[15] N. Martino, P. Feyen, M. Porro, C. Bossio, E. Zucchetti, D. Ghezzi, F. Benfenati, G. Lanzani, M.R. Antognazza, Photothermal cellular stimulation in functional bio-polymer interfaces, Sci. Rep. 5 (2015) 8911.

[16] V. Benfenati, N. Martino, M.R. Antognazza, A. Pistone, S. Toffanin, S. Ferroni, G. Lanzani, M. Muccini, Photostimulation of whole-cell conductance in primary rat neocortical astrocytes mediated by organic semiconducting thin films, Adv. Healthc. Mater. 3 (2014) 392–399.

[17] D. Ghezzi, M.R. Antognazza, M. Dal Maschio, E. Lanzarini, F. Benfenati, G. Lanzani, A hybrid bioorganic interface for neuronal photoactivation, Nat. Commun. 2 (2011) 166.

[18] F. Lodola, V. Vurro, S. Crasto, E. Di Pasquale, G. Lanzani, Optical pacing of human-induced pluripotent stem cell-derived cardiomyocytes mediated by a conjugated polymer interface, Adv. Healthc. Mater. 8 (2019), e1900198.

[19] P. Feyen, E. Colombo, D. Endeman, M. Nova, L. Laudato, N. Martino, M. R. Antognazza, G. Lanzani, F. Benfenati, D. Ghezzi, Light-evoked hyperpolarization and silencing of neurons by conjugated polymers, Sci. Rep. 6 (2016) 22718.

[20] D. Ghezzi, M.R. Antognazza, R. Maccarone, S. Bellani, E. Lanzarini, N. Martino, M. Mete, G. Pertile, S. Bisti, G. Lanzani, F. Benfenati, A polymer optoelectronic interface restores light sensitivity in blind rat retinas, Nat. Photonics 7 (2013) 400–406.

[21] J.F. Maya-Vetencourt, D. Ghezzi, M.R. Antognazza, E. Colombo, M. Mete, P. Feyen, A. Desii, A. Buschiazzo, M. Di Paolo, S. Di Marco, F. Ticconi, L. Emionite, D. Shmal, C. Marini, I. Donelli, G. Freddi, R. Maccarone, S. Bisti, G. Sambuceti, G. Pertile, G. Lanzani, F. Benfenati, A fully organic retinal prosthesis restores vision in a rat model of degenerative blindness, Nat.Mater. 16 (2017) 681–689.

[22] M.R. Antognazza, M. Di Paolo, D. Ghezzi, M. Mete, S. Di Marco, J.F. Maya-Vetencourt, R. Maccarone, A. Desii, F. Di Fonzo, M. Bramini, A. Russo, L. Laudato, I. Donelli, M. Cilli, G. Freddi, G. Pertile, G. Lanzani, S. Bisti, F. Benfenati, Characterization of a polymer-based, fully organic prosthesis for implantation into the subretinal space of the rat, Adv. Healthc. Mater. 5 (2016) 2271–2282.

[23] J.F. Maya-Vetencourt, G. Manfredi, M. Mete, E. Colombo, M. Bramini, S. Di Marco, D. Shmal, G. Mantero, M. Dipalo, A. Rocchi, M.L. DiFrancesco, E. D. Papaleo, A. Russo, J. Barsotti, C. Eleftheriou, F. Di Maria, V. Cossu, F. Piazza, L. Emionite, F. Ticconi, C. Marini, G. Sambuceti, G. Pertile, G. Lanzani, F. Benfenati, Subretinally injected semiconducting polymer nanoparticles rescue vision in a rat model of retinal dystrophy, Nat. Nanotechnol. 15 (2020) 698–708.

[24] C. Bossio, I. Abdel Aziz, G. Tullii, E. Zucchetti, D. Debellis, M. Zangoli, F. Di Maria, G. Lanzani, M.R. Antognazza, Photocatalytic activity of polymer nanoparticles modulates intracellular calcium dynamics and reactive oxygen species in HEK-293 cells, Front. Bioeng. Biotechnol. 6 (2018) 114.

[25] S. Bellani, A. Ghadirzadeh, L. Meda, A. Savoini, A. Tacca, G. Marra, R. Meira, J. Morgado, F. Di Fonzo, M.R. Antognazza, Hybrid organic/inorganic nanostructures for highly sensitive photoelectrochemical detection of dissolved oxygen in aqueous media, Adv. Funct. Mater. 25 (2015) 4531–4538.

[26] S. Negri, P. Faris, R. Berra-Romani, G. Guerra, F. Moccia, Endothelial transient receptor potential channels and vascular remodeling: extracellular Ca(2 +) entry for angiogenesis, arteriogenesis and vasculogenesis, Front. Physiol. 10 (2019) 1618.

[27] F. Lodola, N. Martino, G. Tullii, G. Lanzani, M.R. Antognazza, Conjugated polymers mediate effective activation of the Mammalian Ion Channel Transient Receptor Potential Vanilloid 1, Sci. Rep. 7 (2017) 8477.

[28] M.J. Caterina, M.A. Schumacher, M. Tominaga, T.A. Rosen, J.D. Levine, D. Julius, The capsaicin receptor: a heat-activated ion channel in the pain pathway, Nature 389 (1997) 816–824.

[29] U. Oh, S.W. Hwang, D. Kim, Capsaicin activates a nonselective cation channel in cultured neonatal rat dorsal root ganglion neurons, J. Neurosci. 16 (1996) 1659–1667.

[30] S. Bevan, T. Quallo, D.A. Andersson, Trpv1, Handb. Exp. Pharmacol. 222 (2014) 207–245.

[31] F. Lodola, V. Rosti, G. Tullii, A. Desii, L. Tapella, P. Catarsi, D. Lim, F. Moccia, M. R. Antognazza, Conjugated polymers optically regulate the fate of endothelial colony-forming cells, Sci. Adv. 5 (2019) eaav4620.

[32] M.J. Berridge, M.D. Bootman, H.L. Roderick, Calcium signalling: dynamics, homeostasis and remodelling, Nat. Rev. Mol. Cell Biol. 4 (2003) 517–529.

[33] D.E. Clapham, Calcium signaling, Cell 131 (2007) 1047–1058.

[34] J. Ferreira-Martins, C. Rondon-Clavo, D. Tugal, J.A. Korn, R. Rizzi, M.E. Padin-Iruegas, S. Ottolenghi, A. De Angelis, K. Urbanek, N. Ide-Iwata, D. D'Amario, T. Hosoda, A. Leri, J. Kajstura, P. Anversa, M. Rota, Spontaneous calcium oscillations regulate human cardiac progenitor cell growth, Circ. Res. 105 (2009) 764–774.

[35] A.K. Panda, R. K, A. Gebrekrstos, S. Bose, Y.S. Markandeya, B. Mehta, B. Basu, Tunable Substrate functionalities direct stem cell fate toward electrophysiologically distinguishable neuron-like and glial-like cells, ACS Appl. Mater. Interfaces (2020).

[36] H. Hanna, F.M. Andre, L.M. Mir, Electrical control of calcium oscillations in mesenchymal stem cells using microsecond pulsed electric fields, Stem Cell. Res. Ther. 8 (2017) 91.

[37] A.M. Xu, S.A. Kim, D.S. Wang, A. Aalipour, N.A. Melosh, Temporally resolved direct delivery of second messengers into cells using nanostraws, Lab Chip 16 (2016) 2434–2439.

[38] S. Curcic, O. Tiapko, K. Groschner, Photopharmacology and opto-chemogenetics of TRPC channels-some therapeutic visions, Pharmacol. Ther. 200 (2019) 13–26.

[39] M. Schernthaner, G. Leitinger, H. Wolinski, S.D. Kohlwein, B. Reisinger, R. A. Barb, W.F. Graier, J. Heitz, K. Groschner, Enhanced Ca(2+)entry and tyrosine phosphorylation mediate nanostructure-induced endothelial proliferation, J. Nanomater. (2013), 2013.

[40] F. Moccia, F.A. Ruffinatti, E. Zuccolo, Intracellular Ca(2)(+) signals to reconstruct a broken heart: still a theoretical approach? Curr. Drug Targets 16 (2015) 793–815.

[41] I.A. Aziz, M.R. Antognazza, Wireless nanotechnologies light up the next frontier in cell Calcium signalling, MRS Advances 5 (2020) 3473–3489.

[42] N. Ahamad, B.B. Singh, Calcium channels and their role in regenerative medicine, World J. Stem Cells 13 (2021) 260–280.

[43] F. Moccia, E. Bonetti, S. Dragoni, J. Fontana, F. Lodola, R.B. Romani, U. Laforenza, V. Rosti, F. Tanzi, Hematopoietic progenitor and stem cells circulate by surfing on intracellular Ca2+ waves: a novel target for cell-based therapy and anti-cancer treatment? Curr. Signal Transd. T 7 (2012) 161–176.

[44] F. Moccia, E. Zuccolo, F. Di Nezza, G. Pellavio, P.S. Faris, S. Negri, A. De Luca, U. Laforenza, L. Ambrosone, V. Rosti, G. Guerra, Nicotinic acid adenine dinucleotide phosphate activates two-pore channel TPC1 to mediate lysosomal Ca (2+) release in endothelial colony-forming cells, J. Cell. Physiol. (2020).

[45] F. Lodola, U. Laforenza, F. Cattaneo, F.A. Ruffinatti, V. Poletto, M. Massa, R. Tancredi, E. Zuccolo, A.D. Khdar, A. Riccardi, M. Biggiogera, V. Rosti, G. Guerra, A. Moccia, VEGF-induced intracellular Ca^{2+} oscillations are down-regulated and do not stimulate angiogenesis in breast cancer-derived endothelial colony forming cells, Oncotarget 8 (2017) 95223–95246.

[46] A.P. Thomas, G.S. Bird, G. Hajnoczky, L.D. Robb-Gaspers, J.W. Putney, Spatial and temporal aspects of cellular calcium signaling, FASEB J. 10 (1996) 1505–1517.

[47] R. Berra Romani, A. Raqeeb, U. Laforenza, M.F. Scaffino, F. Moccia, J.E. Avelino-Cruz, A. Oldani, D. Coltrini, V. Milesi, V. Taglietti, F. Tanzi, Cardiac microvascular endothelial cells express a functional Ca+ -sensing receptor, J. Vasc. Res. 46 (2009) 73–82.

[48] G.S. Bird, M.F. Rossier, J.F. Obie, J.W. Putney, Sinusoidal oscillations in intracellular calcium requiring negative feedback by protein kinase C, J. Biol. Chem. 268 (1993) 8425–8428.

[49] F. Moccia, S. Negri, M. Shekha, P. Faris, G. Guerra, Endothelial Ca(2+) signaling, angiogenesis and vasculogenesis: just what it takes to make a blood vessel, Int. J. Mol. Sci. 20 (2019).

[50] Y. Yokota, H. Nakajima, Y. Wakayama, A. Muto, K. Kawakami, S. Fukuhara, N. Mochizuki, Endothelial Ca 2+ oscillations reflect VEGFR signaling-regulated angiogenic capacity in vivo, Elife 4 (2015).

[51] D.P. Noren, W.H. Chou, S.H. Lee, A.A. Qutub, A. Warmflash, D.S. Wagner, A. S. Popel, A. Levchenko, Endothelial cells decode VEGF-mediated Ca2+ signaling patterns to produce distinct functional responses, Sci. Signal 9 (2016) ra20.

[52] S. Dragoni, U. Laforenza, E. Bonetti, F. Lodola, C. Bottino, R. Berra-Romani, G. Carlo Bongio, M.P. Cinelli, G. Guerra, P. Pedrazzoli, V. Rosti, F. Tanzi, F. Moccia, Vascular endothelial growth factor stimulates endothelial colony forming cells proliferation and tubulogenesis by inducing oscillations in intracellular Ca2+ concentration, Stem Cells 29 (2011) 1898–1907.

[53] C. Balbi, K. Lodder, A. Costa, S. Moimas, F. Moccia, T. van Herwaarden, V. Rosti, F. Campagnoli, A. Palmeri, P. De Biasio, F. Santini, M. Giacca, M.J. Goumans, L. Barile, A.M. Smits, S. Bollini, Reactivating endogenous mechanisms of cardiac regeneration via paracrine boosting using the human amniotic fluid stem cell secretome, Int. J. Cardiol. 287 (2019) 87–95.

[54] F. Moccia, Calcium signaling in endothelial colony forming cells in health and disease, Adv. Exp. Med. Biol. 1131 (2020) 1013–1030.

[55] F. Moccia, A. Lucariello, G. Guerra, TRPC3-mediated Ca(2+) signals as a promising strategy to boost therapeutic angiogenesis in failing hearts: the role of autologous endothelial colony forming cells, J. Cell. Physiol. 233 (2018) 3901–3917.

[56] D.J. DelloStritto, P.J. Connell, G.M. Dick, I.S. Fancher, B. Klarich, J.N. Fahmy, P. T. Kang, Y.R. Chen, D.S. Damron, C.K. Thodeti, I.N. Bratz, Differential regulation of TRPV1 channels by H2O2: implications for diabetic microvascular dysfunction, Basic Res. Cardiol. 111 (2016) 21.

[57] P. Faris, F. Ferulli, M. Vismara, M. Tanzi, S. Negri, A. Rumolo, K. Lefkimmiatis, M. Maestri, M. Shekha, P. Pedrazzoli, G.F. Guidetti, D. Montagna, F. Moccia, Hydrogen sulfide-evoked intracellular Ca(2+) signals in primary cultures of metastatic colorectal cancer cells, Cancers (Basel) 12 (2020).

[58] S. Song, R.J. Ayon, A. Yamamura, H. Yamamura, S. Dash, A. Babicheva, H. Tang, X. Sun, A.G. Cordery, Z. Khalpey, S.M. Black, A.A. Desai, F. Rischard, K. M. McDermott, J.G. Garcia, A. Makino, J.X. Yuan, Capsaicin-induced Ca(2+) signaling is enhanced via upregulated TRPV1 channels in pulmonary artery smooth muscle cells from patients with idiopathic PAH, Am. J. Physiol. Lung Cell Mol. Physiol. 312 (2017) L309–L325.

[59] T. Stueber, M.J. Eberhardt, Y. Caspi, S. Lev, A. Binshtok, A. Leffler, Differential cytotoxicity and intracellular calcium-signalling following activation of the calcium-permeable ion channels TRPV1 and TRPA1, Cell Calcium 68 (2017) 34–44.

[60] G. Guarini, V.A. Ohanyan, J.G. Kmetz, D.J. DelloStritto, R.J. Thoppil, C. K. Thodeti, J.G. Meszaros, D.S. Damron, I.N. Bratz, Disruption of TRPV1-mediated coupling of coronary blood flow to cardiac metabolism in diabetic mice: role of nitric oxide and BK channels, Am. J. Physiol. Heart Circ. Physiol. 303 (2012) H216–H223.

[61] F. Andrade, C. Rangel-Sandoval, A. Rodriguez-Hernandez, E. Lopez-Dyck, A. Elizalde, A. Virgen-Ortiz, E. Bonales-Alatorre, G. Valencia-Cruz, E. Sanchez-Pastor, Capsaicin causes vasorelaxation of rat aorta through blocking of L-type Ca (2+) channels and activation of CB1 receptors, Molecules 25 (2020).

[62] M. Gryszel, M. Sytnyk, M. Jakesova, G. Romanazzi, R. Gabrielsson, W. Heiss, E. D. Glowacki, General observation of photocatalytic oxygen reduction to hydrogen peroxide by organic semiconductor thin films and colloidal crystals, ACS Appl. Mater. Interfaces 10 (2018) 13253–13257.

[63] S. Martinotti, U. Laforenza, M. Patrone, F. Moccia, E. Ranzato, Honey-mediated wound healing: H(2)O(2) entry through AQP3 determines extracellular Ca(2+) influx, Int. J. Mol. Sci. 20 (2019).

[64] H.H. Chuang, S. Lin, Oxidative challenges sensitize the capsaicin receptor by covalent cysteine modification, Proc. Natl. Acad. Sci. U. S. A. 106 (2009) 20097–20102.

[65] K. Susankova, K. Tousova, L. Vyklicky, J. Teisinger, V. Vlachova, Reducing and oxidizing agents sensitize heat-activated vanilloid receptor (TRPV1) current, Mol. Pharmacol. 70 (2006) 383–394.

[66] S.P. Didion, F.M. Faraci, Effects of NADH and NADPH on superoxide levels and cerebral vascular tone, Am. J. Physiol. Heart Circ. Physiol. 282 (2002) H688–H695.

[67] M.N. Sullivan, A.L. Gonzales, P.W. Pires, A. Bruhl, M.D. Leo, W. Li, A. Oulidi, F. A. Boop, Y. Feng, J.H. Jaggar, D.G. Welsh, S. Earley, Localized TRPA1 channel Ca2+ signals stimulated by reactive oxygen species promote cerebral artery dilation, Sci. Signal. 8 (2015) ra2.

[68] M.Y. Song, A. Makino, J.X. Yuan, Role of reactive oxygen species and redox in regulating the function of transient receptor potential channels, Antioxid. Redox Signal. 15 (2011) 1549–1565.

[69] D.A. Andersson, C. Gentry, S. Moss, S. Bevan, Transient receptor potential A1 is a sensory receptor for multiple products of oxidative stress, J. Neurosci. 28 (2008) 2485–2494.

[70] P.J. Bartlett, I. Cloete, J. Sneyd, A.P. Thomas, IP3-dependent Ca(2+) oscillations switch into a dual oscillator mechanism in the presence of PLC-linked hormones, iScience 23 (2020), 101062.

[71] R. Berra-Romani, A. Raqeeb, J. Torres-Jácome, A. Guzman-Silva, G. Guerra, F. Tanzi, F. Moccia, The mechanism of injury-induced intracellular calcium concentration oscillations in the endothelium of excised rat aorta, J. Vasc. Res. 49 (2012) 65–76.

[72] F. Moccia, E. Zuccolo, F. Di Nezza, G. Pellavio, P.S. Faris, S. Negri, A. De Luca, U. Laforenza, L. Ambrosone, V. Rosti, G. Guerra, Nicotinic acid adenine dinucleotide phosphate activates two-pore channel TPC1 to mediate lysosomal Ca (2+) release in endothelial colony-forming cells, J. Cell. Physiol. 236 (2021) 688–705.

[73] A.B. Parekh, R. Penner, Activation of store-operated calcium influx at resting InsP3 levels by sensitization of the InsP3 receptor in rat basophilic leukaemia cells, J. Physiol. 489 (Pt 2) (1995) 377–382.

[74] M. Gericke, G. Droogmans, B. Nilius, Thimerosal induced changes of intracellular calcium in human endothelial cells, Cell Calcium 14 (1993) 201–207.

[75] M.D. Bootman, C.W. Taylor, M.J. Berridge, The thiol reagent, thimerosal, evokes Ca2+ spikes in HeLa cells by sensitizing the inositol 1,4,5-trisphosphate receptor, J. Biol. Chem. 267 (1992) 25113–25119.

[76] F. Moccia, S. Dragoni, F. Lodola, E. Bonetti, C. Bottino, G. Guerra, U. Laforenza, V. Rosti, F. Tanzi, Store-dependent Ca(2+) entry in endothelial progenitor cells as a perspective tool to enhance cell-based therapy and adverse tumour vascularization, Curr. Med. Chem. 19 (2012) 5802–5818.

[77] Y. Sanchez-Hernandez, U. Laforenza, E. Bonetti, J. Fontana, S. Dragoni, M. Russo, J.E. Avelino-Cruz, S. Schinelli, D. Testa, G. Guerra, V. Rosti, F. Tanzi, F. Moccia, Store-operated Ca(2+) entry is expressed in human endothelial progenitor cells, Stem Cells Dev. 19 (2010) 1967–1981.

[78] F. Lodola, U. Laforenza, E. Bonetti, D. Lim, S. Dragoni, C. Bottino, H.L. Ong, G. Guerra, C. Ganini, M. Massa, M. Manzoni, I.S. Ambudkar, A.A. Genazzani, V. Rosti, P. Pedrazzoli, F. Tanzi, F. Moccia, C. Porta, Store-operated Ca2+ entry is remodelled and controls in vitro angiogenesis in endothelial progenitor cells isolated from tumoral patients, PLoS ONE 7 (2012) e42541.

[79] F. Moccia, E. Zuccolo, V. Poletto, I. Turin, G. Guerra, P. Pedrazzoli, V. Rosti, C. Porta, D. Montagna, Targeting Stim and Orai proteins as an alternative approach in anticancer therapy, Curr. Med. Chem. 23 (2016) 3450–3480.

[80] I. Abdel Aziz, M. Malferrari, F. Roggiani, G. Tullii, S. Rapino, M.R. Antognazza, Light-Triggered electron transfer between a conjugated polymer and cytochrome C for optical modulation of redox signaling, iScience 23 (2020), 101091.

[81] V. Balducci, P. Faris, C. Balbi, A. Costa, S. Negri, V. Rosti, S. Bollini, F. Moccia, The human amniotic fluid stem cell secretome triggers intracellular Ca(2+) oscillations, NF-kappaB nuclear translocation and tube formation in human endothelial colony-forming cells, J. Cell. Mol. Med. 25 (2021) 8074–8086.

[82] Y.S. Maeng, H.J. Choi, J.Y. Kwon, Y.W. Park, K.S. Choi, J.K. Min, Y.H. Kim, P. G. Suh, K.S. Kang, M.H. Won, Y.M. Kim, Y.G. Kwon, Endothelial progenitor cell homing: prominent role of the IGF2-IGF2R-PLCbeta2 axis, Blood 113 (2009) 233–243.

[83] P.V. Peplow, T.Y. Chung, G.D. Baxter, Laser photobiomodulation of proliferation of cells in culture: a review of human and animal studies, Photomed. Laser Surg. 28 (2010). Suppl 1S3-40.

[84] E. Zucchetti, M. Zangoli, I. Bargigia, C. Bossio, F. Di Maria, G. Barbarella, C. D'Andrea, G. Lanzani, M.R. Antognazza, Poly(3-hexylthiophene) nanoparticles for biophotonics: study of the mutual interaction with living cells, J. Mater. Chem. B 5 (2017) 565–574.

[85] N.A. Hofmann, S. Barth, M. Waldeck-Weiermair, C. Klec, D. Strunk, R. Malli, W. F. Graier, TRPV1 mediates cellular uptake of anandamide and thus promotes endothelial cell proliferation and network-formation, Biol. Open 3 (2014) 1164–1172.

[86] N. Kedei, T. Szabo, J.D. Lile, J.J. Treanor, Z. Olah, M.J. Iadarola, P.M. Blumberg, Analysis of the native quaternary structure of vanilloid receptor 1, J. Biol. Chem. 276 (2001) 28613–28619.

[87] N.A. Veldhuis, M.J. Lew, F.C. Abogadie, D.P. Poole, E.A. Jennings, J.J. Ivanusic, H. Eilers, N.W. Bunnett, P. McIntyre, N-glycosylation determines ionic permeability and desensitization of the TRPV1 capsaicin receptor, J. Biol. Chem. 287 (2012) 21765–21772.

[88] R. Chen, G. Romero, M.G. Christiansen, A. Mohr, P. Anikeeva, Wireless magnetothermal deep brain stimulation, Science 347 (2015) 1477–1480.

[89] D. Nelidova, R.K. Morikawa, C.S. Cowan, Z. Raics, D. Goldblum, H.P.N. Scholl, T. Szikra, A. Szabo, D. Hillier, B. Roska, Restoring light sensitivity using tunable near-infrared sensors, Science 368 (2020) 1108–1113.

[90] A. Gomes, E. Fernandes, J.L. Lima, Fluorescence probes used for detection of reactive oxygen species, J. Biochem. Biophys. Methods 65 (2005) 45–80.

[91] Q. Hu, S. Corda, J.L. Zweier, M.C. Capogrossi, R.C. Ziegelstein, Hydrogen peroxide induces intracellular calcium oscillations in human aortic endothelial cells, Circulation 97 (1998) 268–275.

[92] Y. Zheng, X. Shen, H2O2 Directly Activates Inositol 1,4,5-trisphosphate Receptors in Endothelial Cells, 10, Redox report: communications in free radical research, 2005, pp. 29–36.

[93] P.V. Avdonin, A.D. Nadeev, G.Y. Mironova, I.L. Zharkikh, P.P. Avdonin, N. V. Goncharov, Enhancement by hydrogen peroxide of calcium signals in endothelial cells induced by 5-HT1B and 5-HT2B receptor agonists, Oxid. Med. Cell. Longev. (2019), 1701478, 2019.

[94] P.W. Pires, S. Earley, Redox regulation of transient receptor potential channels in the endothelium, Microcirculation 24 (2017).

[95] N.Y. Hakami, A.K. Ranjan, A.A. Hardikar, G.J. Dusting, H.M. Peshavariya, Role of NADPH oxidase-4 in human endothelial progenitor cells, Front. Physiol. 8 (2017) 150.

[96] D.J. DelloStritto, P. Sinharoy, P.J. Connell, J.N. Fahmy, H.C. Cappelli, C. K. Thodeti, W.J. Geldenhuys, D.S. Damron, I.N. Bratz, 4-Hydroxynonenal dependent alteration of TRPV1-mediated coronary microvascular signaling, Free Radic, Biol. Med. 101 (2016) 10–19.

[97] S. Negri, P. Faris, F. Moccia, Reactive oxygen species and endothelial Ca(2+) signaling: brothers in arms or partners in crime? Int. J. Mol. Sci. 22 (2021).

[98] S. Negri, P. Faris, T. Soda, F. Moccia, Endothelial signaling at the core of neurovascular coupling: the emerging role of endothelial inward-rectifier K(+) (Kir2.1) channels and N-methyl-D-aspartate receptors in the regulation of cerebral blood flow, Int. J. Biochem. Cell Biol. 135 (2021), 105983.

[99] R. Ding, Y.L. Yin, L.H. Jiang, Reactive oxygen species-induced TRPM2-mediated Ca(2+) signalling in endothelial cells, Antioxidants 10 (2021).
[100] H.R. Heathcote, M.D. Lee, X. Zhang, C.D. Saunter, C. Wilson, J.G. McCarron, Endothelial TRPV4 channels modulate vascular tone by Ca(2+) -induced Ca(2+) release at inositol 1,4,5-trisphosphate receptors, Br. J. Pharmacol. 176 (2019) 3297–3317.
[101] A.J. Morgan, R. Jacob, Ca2+ influx does more than provide releasable Ca2+ to maintain repetitive spiking in human umbilical vein endothelial cells, Biochem. J. 320 (Pt 2) (1996) 505–517.
[102] S.K. Joseph, Role of thiols in the structure and function of inositol trisphosphate receptors, Curr. Top. Membr. 66 (2010) 299–322.
[103] F. Moccia, F. Lodola, I. Stadiotti, C.A. Pilato, M. Bellin, S. Carugo, G. Pompilio, E. Sommariva, A.S. Maione, Calcium as a key player in arrhythmogenic cardiomyopathy: adhesion disorder or intracellular alteration? Int. J. Mol. Sci. 20 (2019).
[104] M. Malferrari, M. Becconi, S. Rapino, Electrochemical monitoring of reactive oxygen/nitrogen species and redox balance in living cells, Anal. Bioanal. Chem. 411 (2019) 4365–4374.
[105] J.H. Hong, S.J. Moon, H.M. Byun, M.S. Kim, H. Jo, Y.S. Bae, S.I. Lee, M. D. Bootman, H.L. Roderick, D.M. Shin, J.T. Seo, Critical role of phospholipase Cgamma1 in the generation of H2O2-evoked [Ca2+]i oscillations in cultured rat cortical astrocytes, J. Biol. Chem. 281 (2006) 13057–13067.
[106] G. Guerra, A. Lucariello, A. Perna, L. Botta, A. De Luca, F. Moccia, The role of endothelial Ca(2+) signaling in neurovascular coupling: a view from the lumen, Int. J Mol. Sci. 19 (2018) pii: E938.
[107] X. Zhang, M.D. Lee, C. Wilson, J.G. McCarron, Hydrogen peroxide depolarizes mitochondria and inhibits IP3-evoked Ca(2+) release in the endothelium of intact arteries, Cell Calcium 84 (2019), 102108.
[108] M.J. Berridge, Remodelling Ca2+ signalling systems and cardiac hypertrophy, Biochem. Soc. Trans. 34 (2006) 228–231.
[109] J. McDaid, S. Mustaly-Kalimi, G.E. Stutzmann, Ca(2+) Dyshomeostasis disrupts neuronal and synaptic function in Alzheimer's disease, Cells 9 (2020).
[110] L. Tapella, T. Soda, L. Mapelli, V. Bortolotto, H. Bondi, F.A. Ruffinatti, G. Dematteis, A. Stevano, M. Dionisi, S. Ummarino, A. Di Ruscio, C. Distasi, M. Grilli, A.A. Genazzani, E. D'Angelo, F. Moccia, D. Lim, Deletion of calcineurin from GFAP-expressing astrocytes impairs excitability of cerebellar and hippocampal neurons through astroglial Na(+) /K(+) ATPase, Glia 68 (2020) 543–560.
[111] R. Silva-Rojas, J. Laporte, J. Bohm, STIM1/ORAI1 loss-of-function and gain-of-function mutations inversely impact on SOCE and calcium homeostasis and cause multi-systemic mirror diseases, Front. Physiol. 11 (2020), 604941.
[112] C. Wilson, X. Zhang, M.D. Lee, M. MacDonald, H.R. Heathcote, N.M.N. Alorfi, C. Buckley, S. Dolan, J.G. McCarron, Disrupted endothelial cell heterogeneity and network organization impair vascular function in prediabetic obesity, Metabolism (2020), 154340.
[113] E.C. Peters, M.T. Gee, L.N. Pawlowski, A.M. Kath, F.D. Polk, C.J. Vance, J. L. Sacoman, P.W. Pires, Amyloid-beta disrupts unitary calcium entry through endothelial NMDA receptors in mouse cerebral arteries, J. Cereb. Blood Flow Metab. (2021), 271678X211039592.
[114] V. Lionetti, S. Bollini, R. Coppini, A. Gerbino, A. Ghigo, G. Iaccarino, R. Madonna, F. Mangiacapra, M. Miragoli, F. Moccia, L. Munaron, P. Pagliaro, A. Parenti, T. Pasqua, C. Penna, F. Quaini, C. Rocca, M. Samaja, L. Sartiani, T. Soda, C. G. Tocchetti, T. Angelone, Understanding the heart-brain axis response in COVID-19 patients: a suggestive perspective for therapeutic development, Pharmacol. Res. 168 (2021), 105581.